Supporting Information

Complexation of Triptycene-Derived Macrotricyclic Polyether with Paraquat Derivatives, Diquat and a 2,7-Diazapyrenium Salt: Guests Induced Conformational Changes of the Host

Ying Han,[a,b] Jing Cao,[a] Peng-Fei Li,[a,b] Qian-Shou Zong,[a] Jian-Min Zhao,[a] Jia-Bin Guo,[a] Jun-Feng Xiang,[a] and Chuan-Feng Chen[a],*

[a] Beijing National Laboratory for Molecular Sciences, CAS Key Laboratory of Molecular Recognition and Function, Institute of Chemistry, Chinese Academy of Sciences, Beijing 100190, China.

[b] University of Chinese Academy of Sciences, Beijing 100049, China.

E-mail: cchen@iccas.ac.cn

Contents

1. ^{1}H NMR and ^{13}C NMR spectra of new compounds

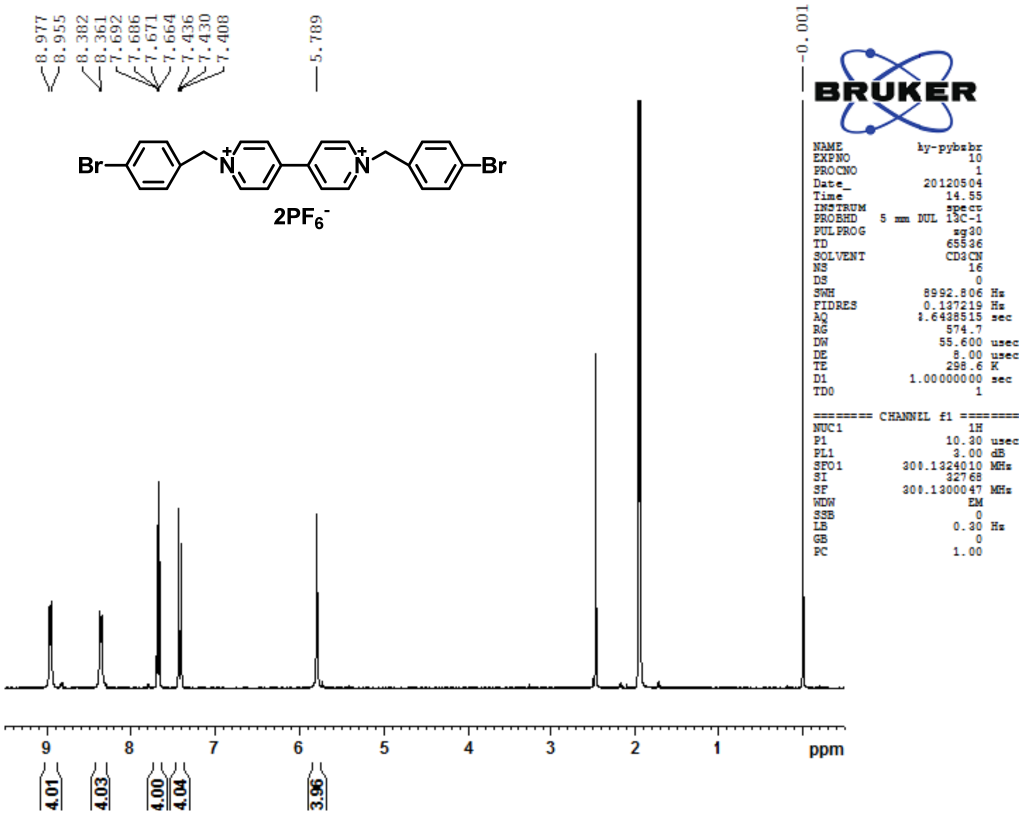

Figure S1. ^{1}H NMR spectrum (300 MHz, CD_3CN) of **8**.

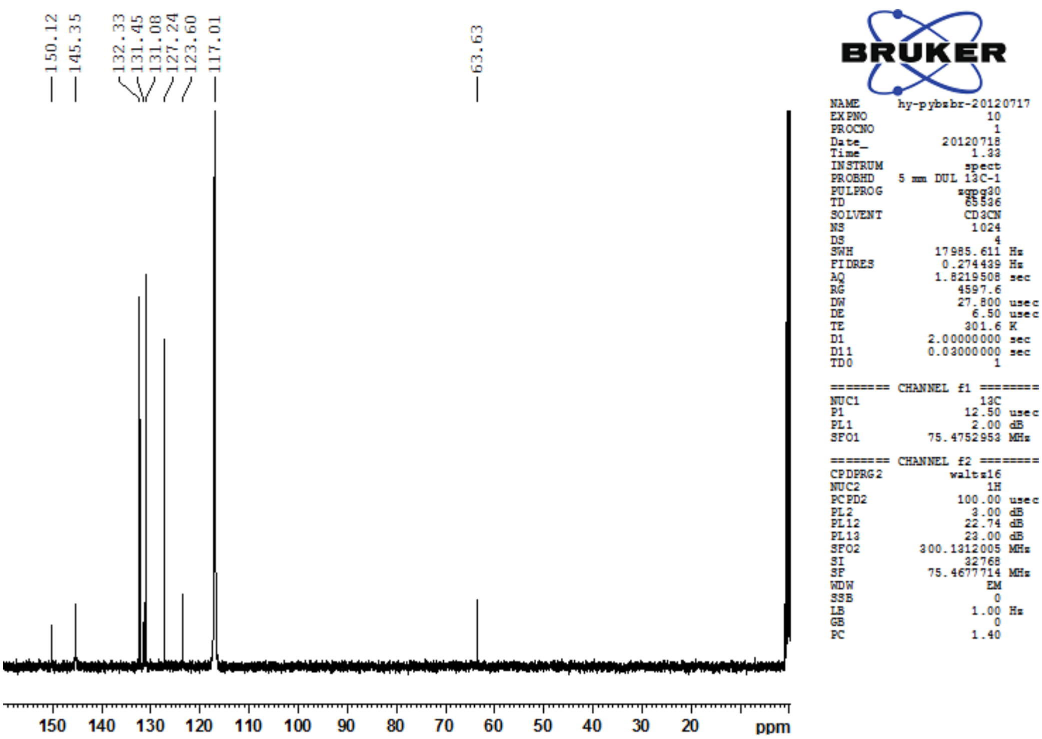

Figure S2. ^{13}C NMR spectrum (75 MHz, CD_3CN) of **8**.

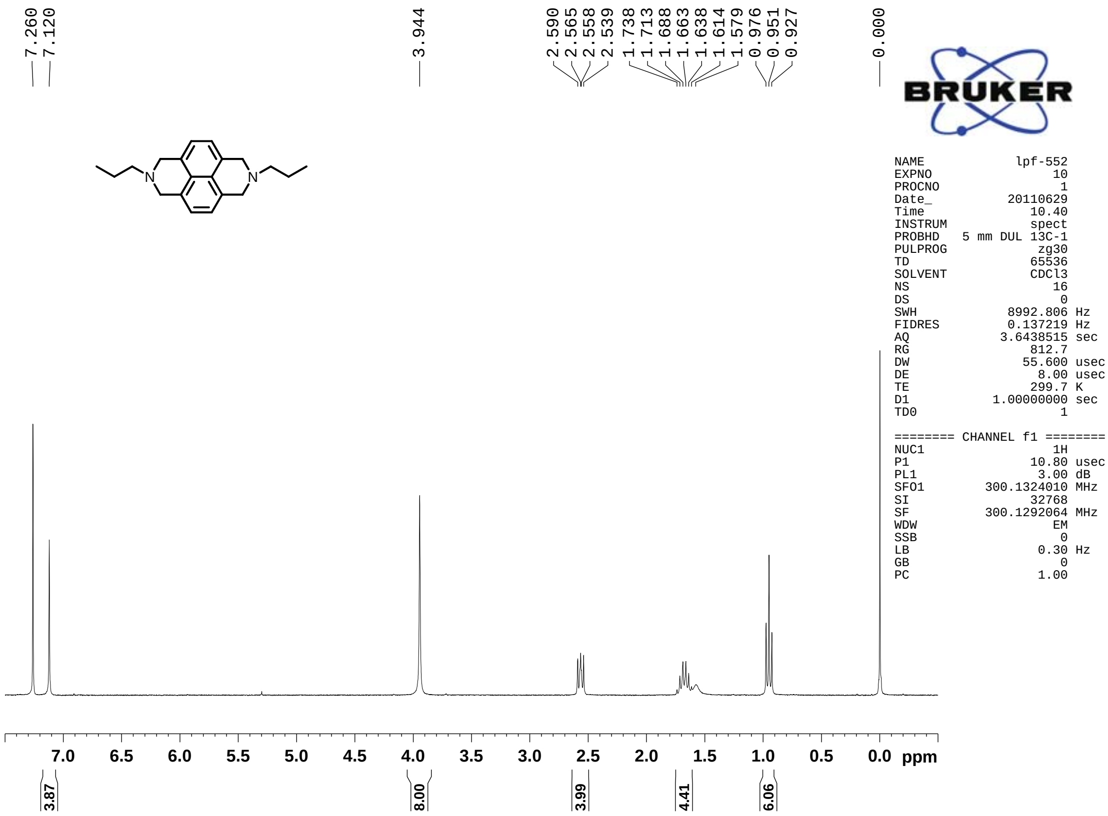

Figure S3. ^{1}H NMR spectrum (300 MHz, $CDCl_3$) of **12**.

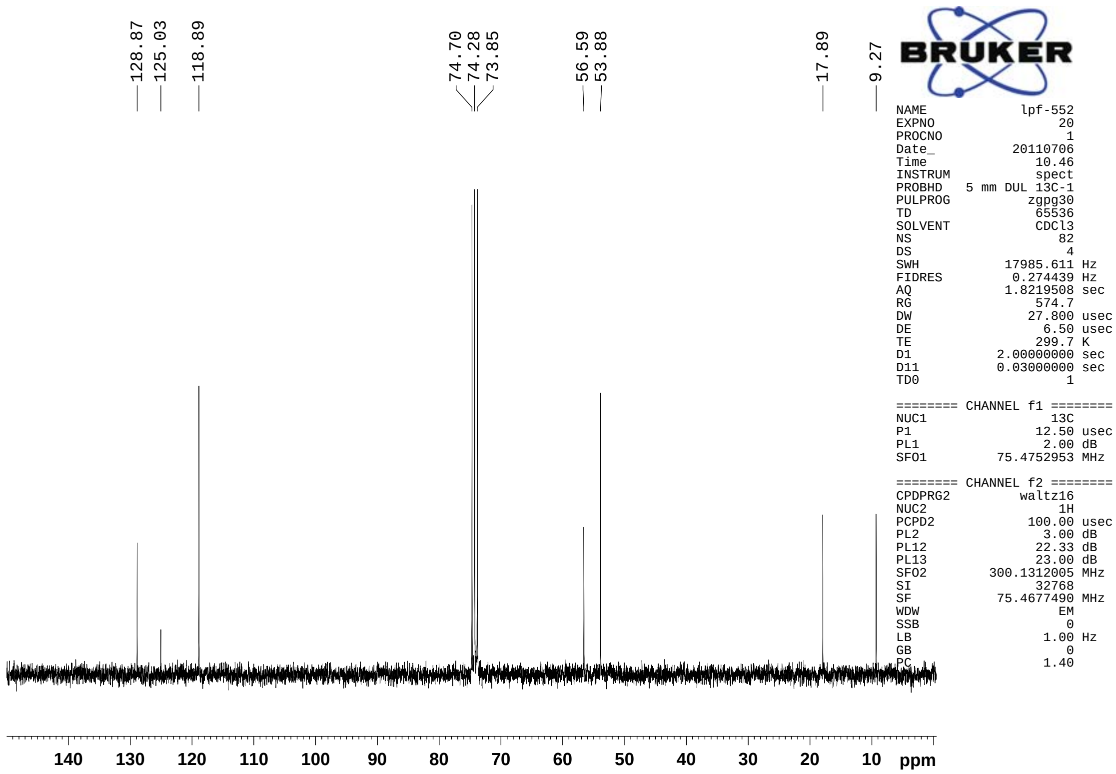

Figure S4. ^{13}C NMR spectrum (75 MHz, $CDCl_3$) of **12**.

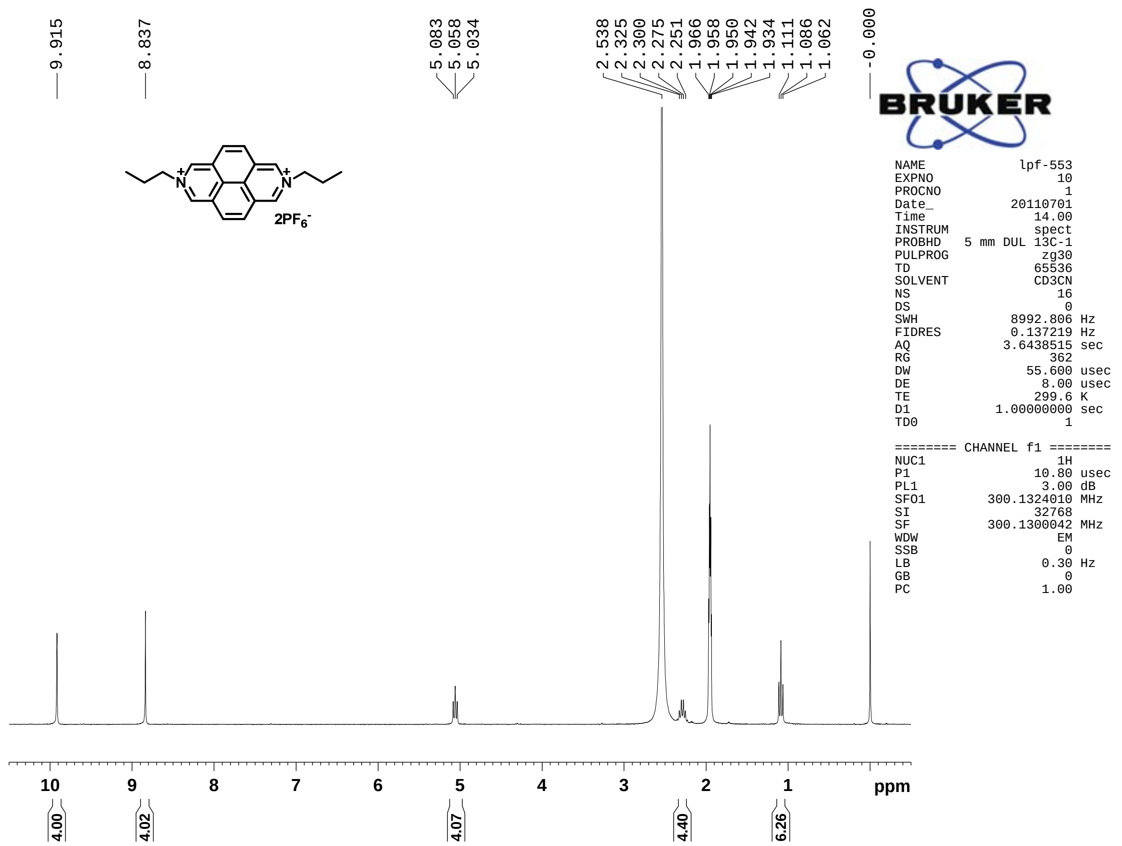

Figure S5. ^{1}H NMR spectrum (300 MHz, CD_3CN) of **11**.

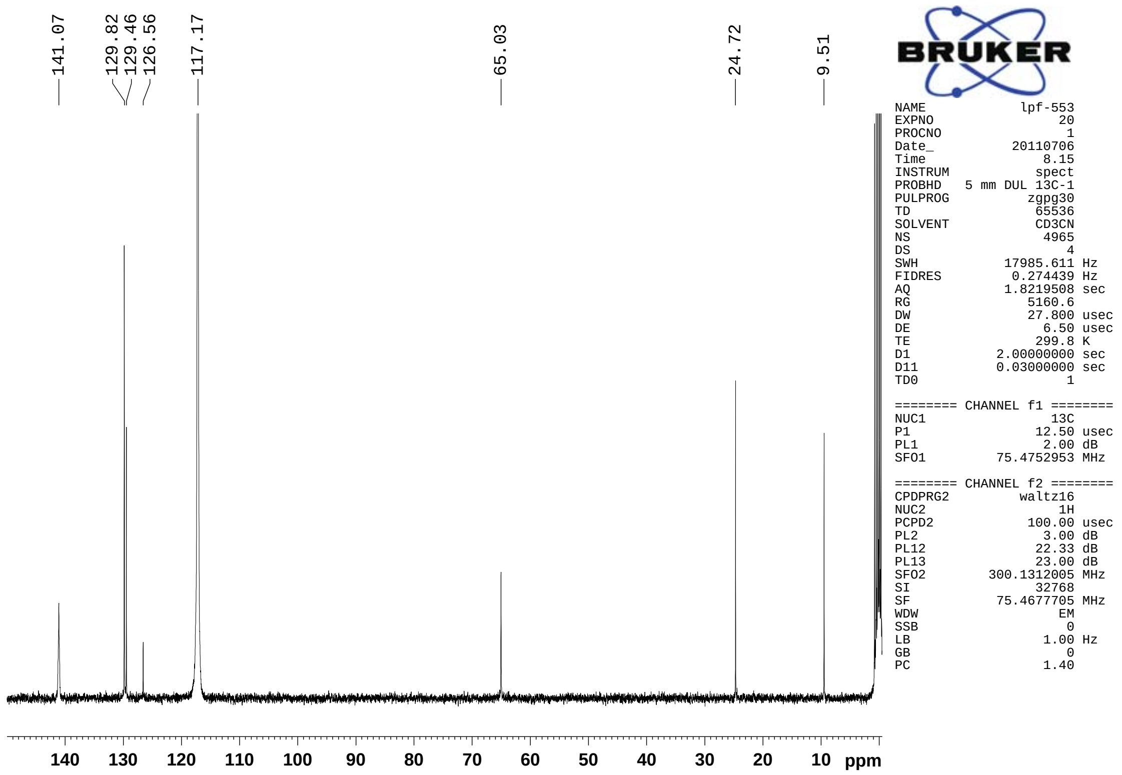

Figure S6. ^{13}C NMR spectrum (75 MHz, CD_3CN) of **11**.

2. ^{1}H NMR spectroscopic titrations of the complexes

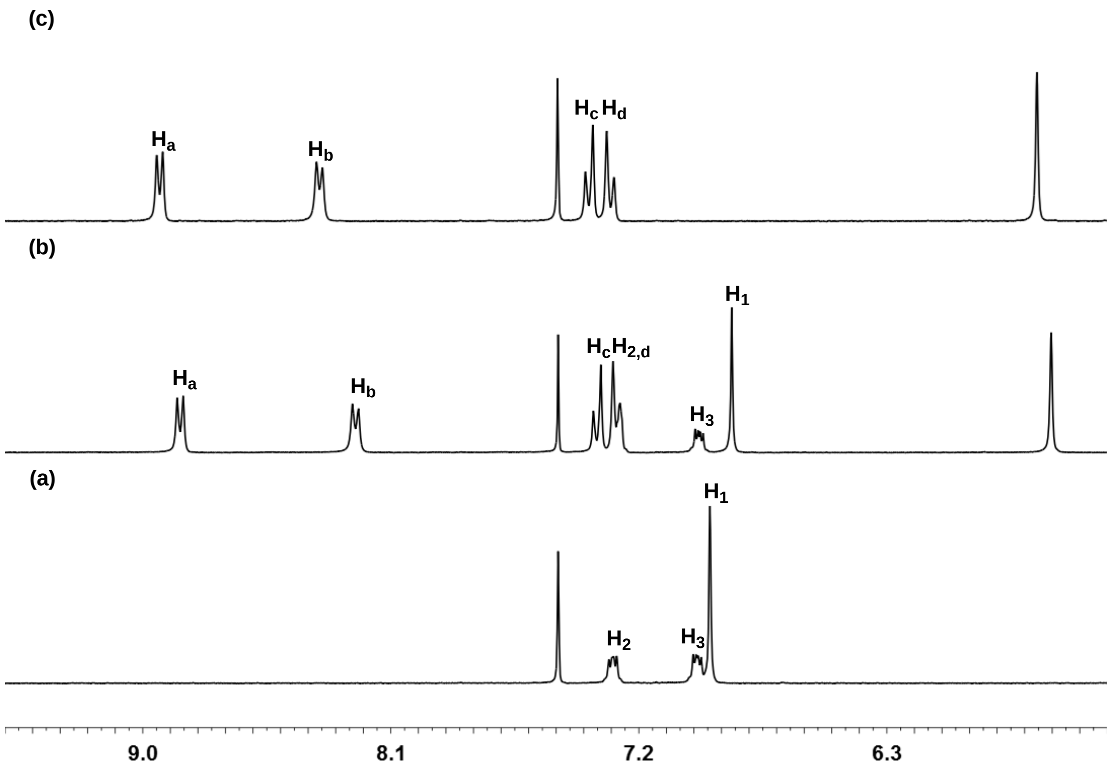

Figure S7. Partial ^{1}H NMR spectra (300 MHz, $CD_3CN/CDCl_3 = 1{:}1$, 298 K) of (a) free **1**, (b) **1** and 1.0 equiv of **5**, (c) free **5**. $[\mathbf{1}]_0 = 3.0$ mM.

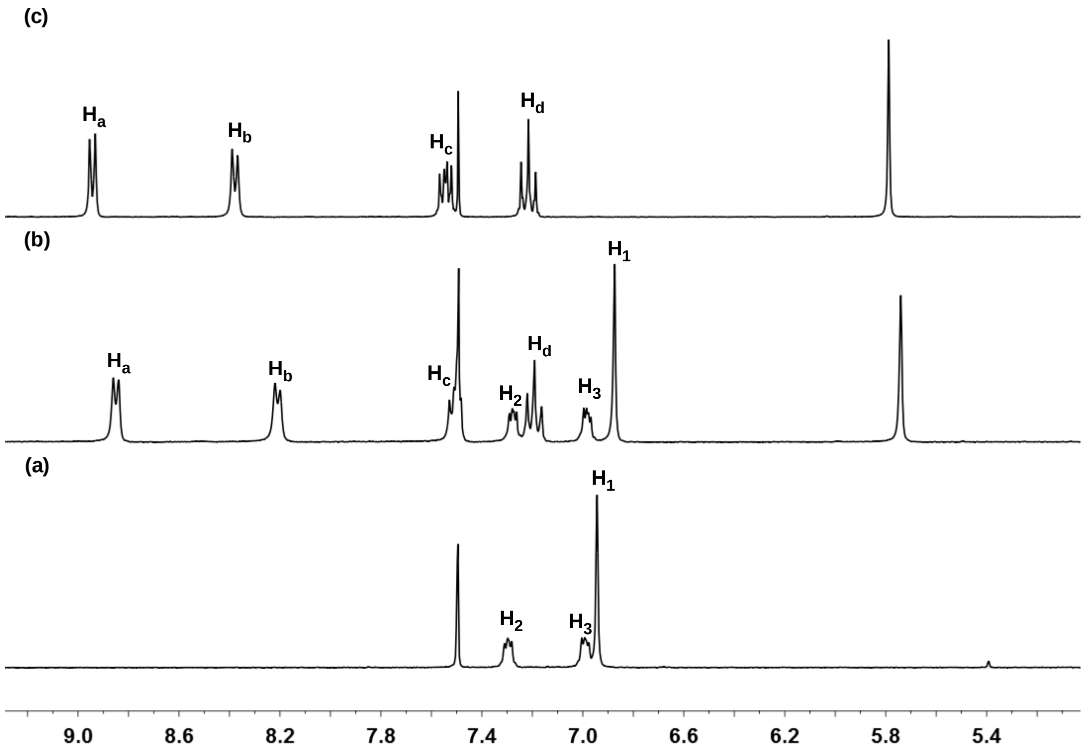

Figure S8. Partial ^{1}H NMR spectra (300 MHz, $CD_3CN/CDCl_3 = 1{:}1$, 298 K) of (a) free **1**, (b) **1** and 1.0 equiv of **6**, (c) free **6**. $[\mathbf{1}]_0 = 3.0$ mM.

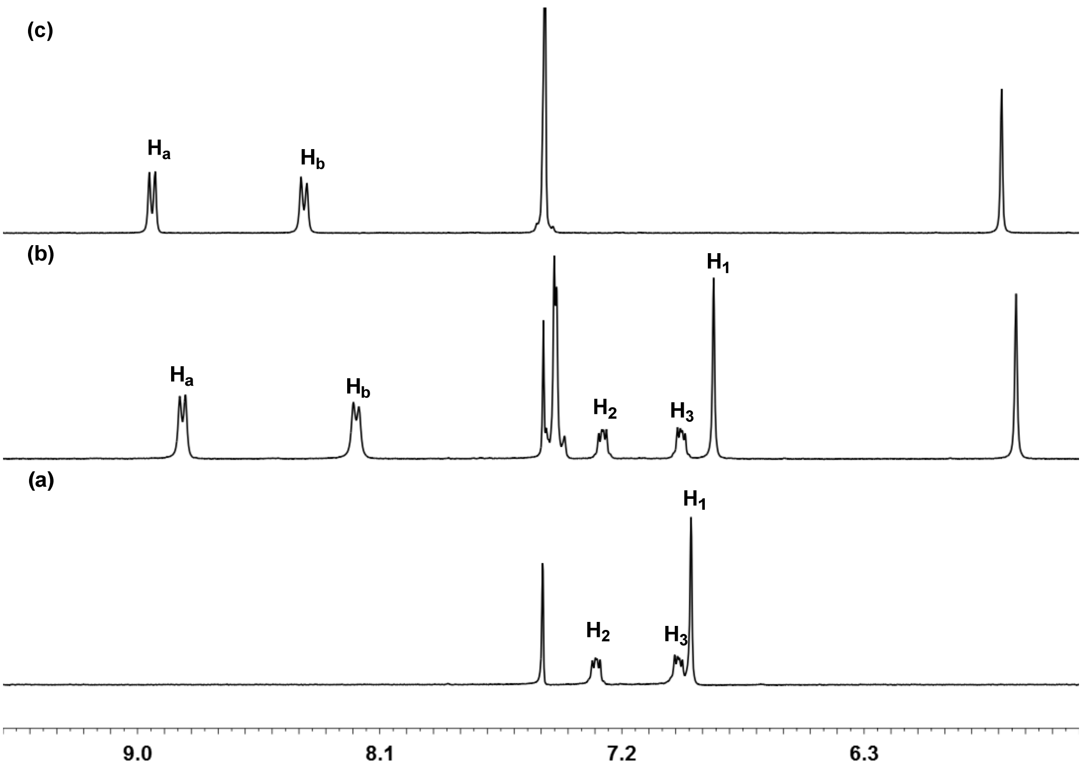

Figure S9. Partial ^{1}H NMR spectra (300 MHz, $CD_3CN/CDCl_3$ = 1:1, 298 K) of (a) free **1**, (b) **1** and 1.0 equiv of **7**, (c) free **7**. $[\mathbf{1}]_0$ = 3.0 mM.

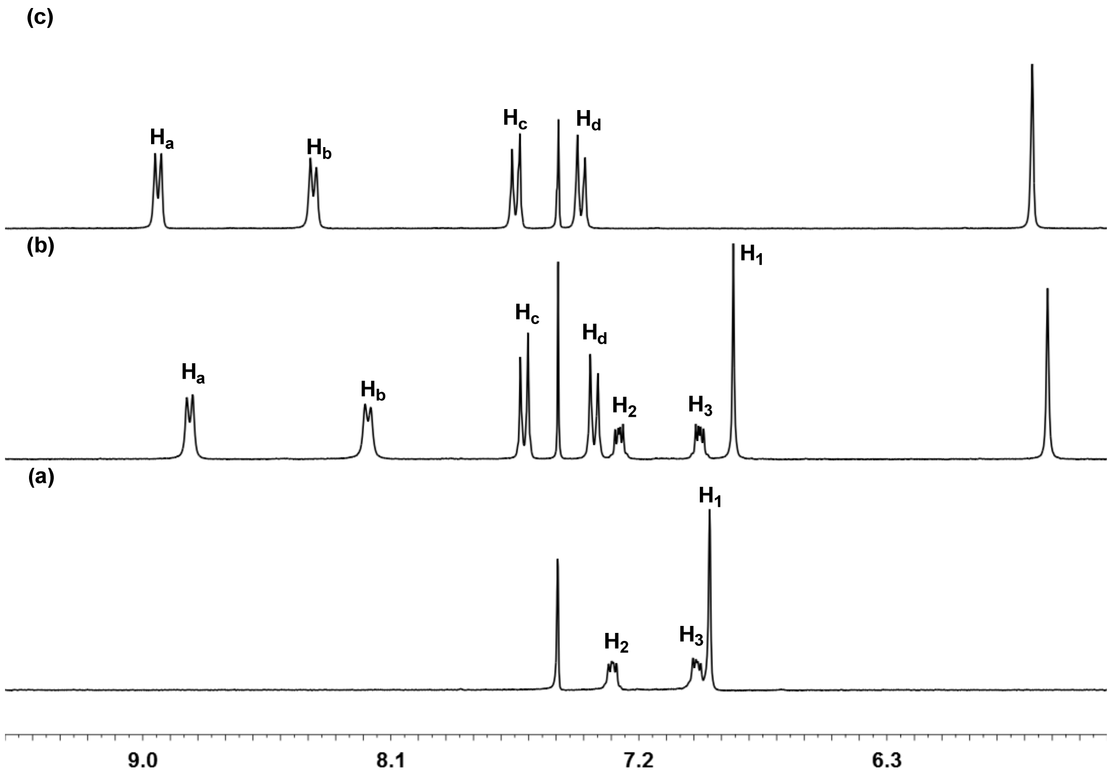

Figure S10. Partial ^{1}H NMR spectra (300 MHz, $CD_3CN/CDCl_3$ = 1:1, 298 K) of (a) free **1**, (b) **1** and 1.0 equiv of **8**, (c) free **8**. $[\mathbf{1}]_0$ = 3.0 mM.

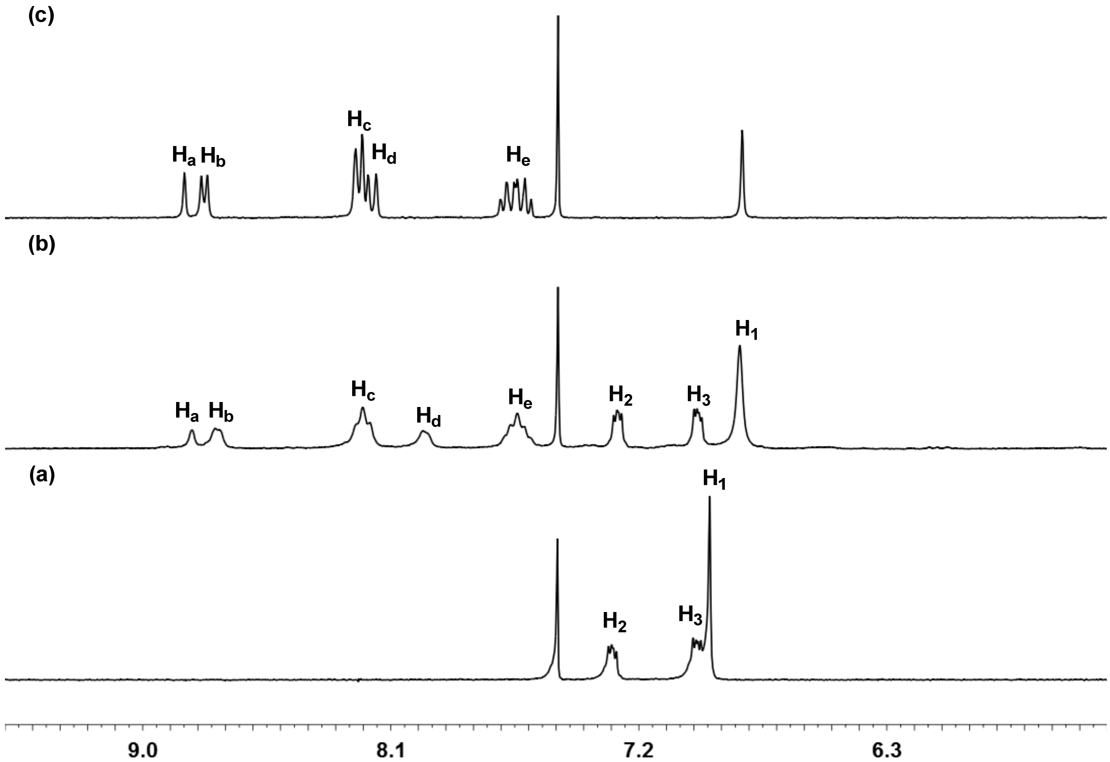

Figure S11. Partial ^{1}H NMR spectra (300 MHz, $CD_3CN/CDCl_3$ = 1:1, 298 K) of (a) free **1**, (b) **1** and 1.0 equiv of **9**, (c) free **9**. $[\mathbf{1}]_0$ = 3.0 mM.

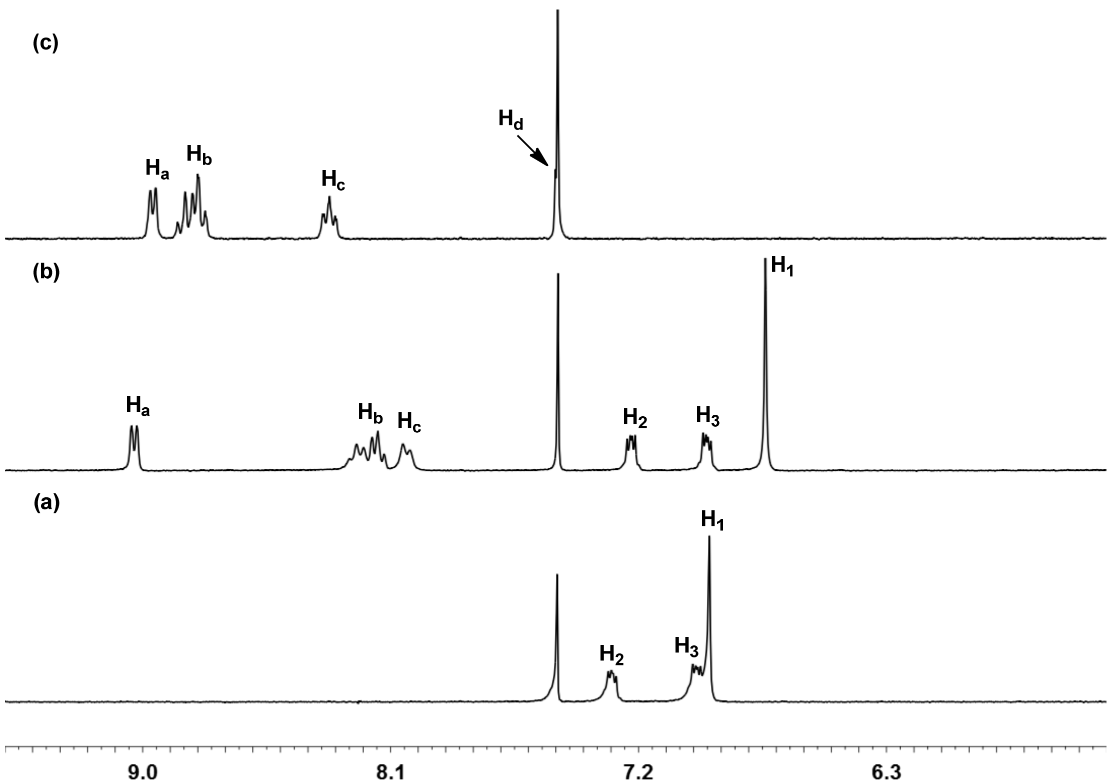

Figure S12. Partial ^{1}H NMR spectra (300 MHz, $CD_3CN/CDCl_3$ = 1:1, 298 K) of (a) free **1**, (b) **1** and 1.0 equiv of **10**, (c) free **10**. $[\mathbf{1}]_0$ = 3.0 mM.

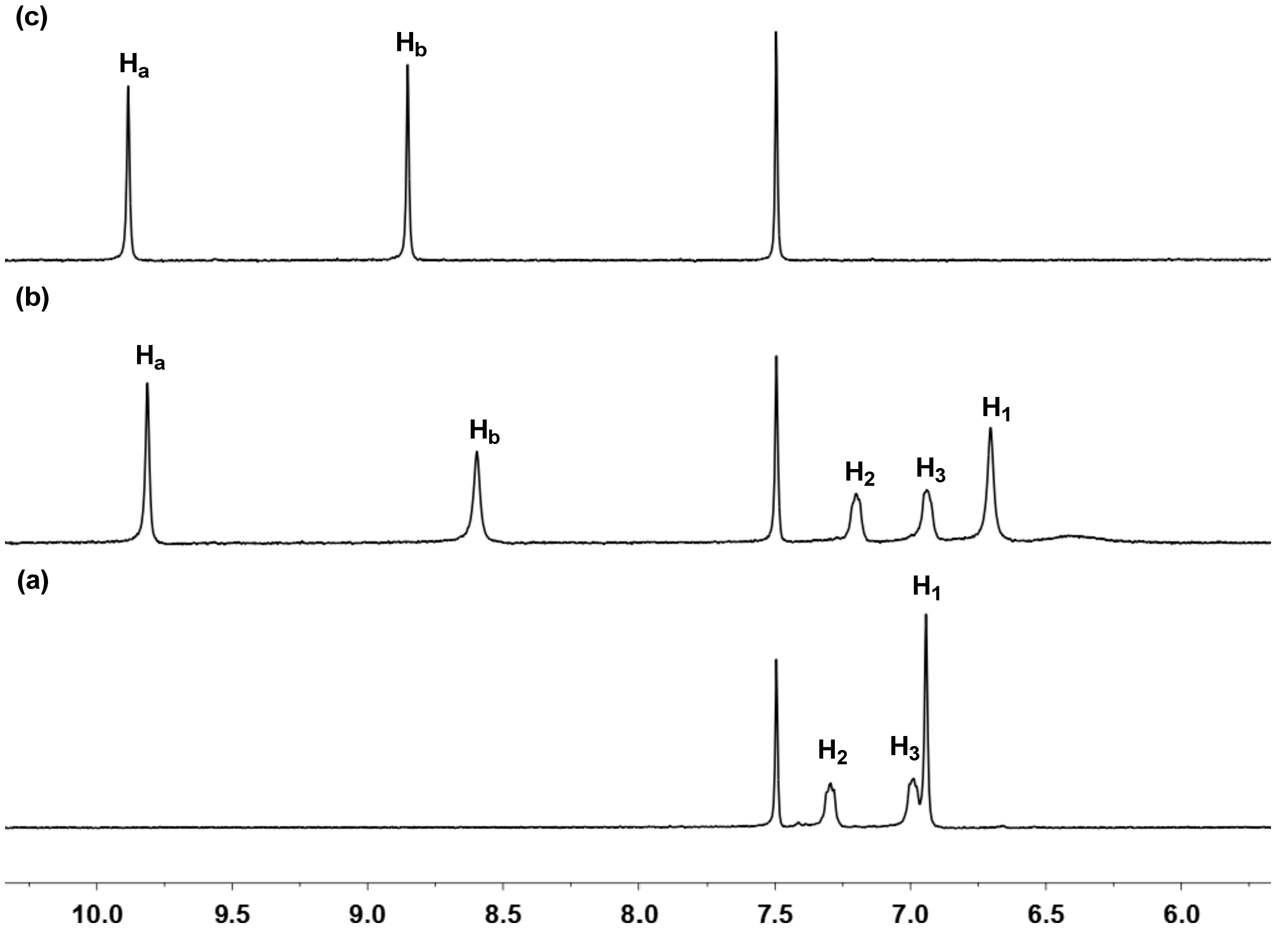

Figure S13. Partial [1]H NMR spectra (300 MHz, $CD_3CN/CDCl_3$ = 1:1, 298 K) of (a) free **1**, (b) **1** and 1.0 equiv of **11**, (c) free **11**. [**1**]$_0$ = 3.0 mM.

3. ^1H-^1H COSY and ROESY NMR spectra of the complexes

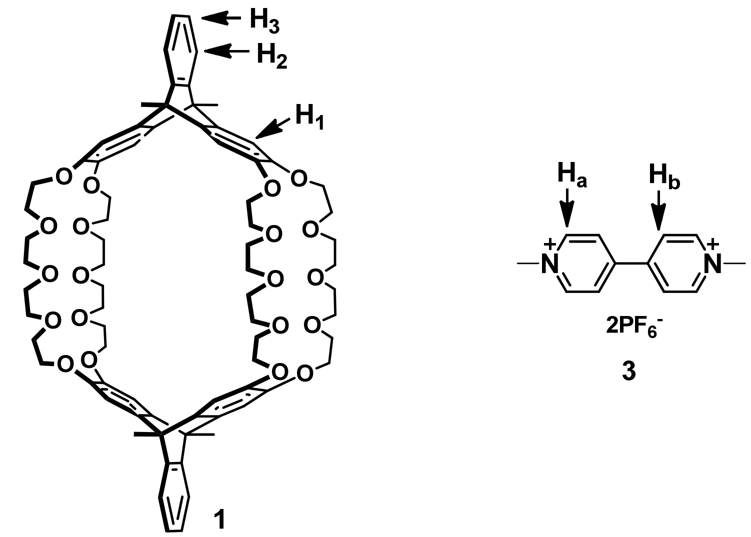

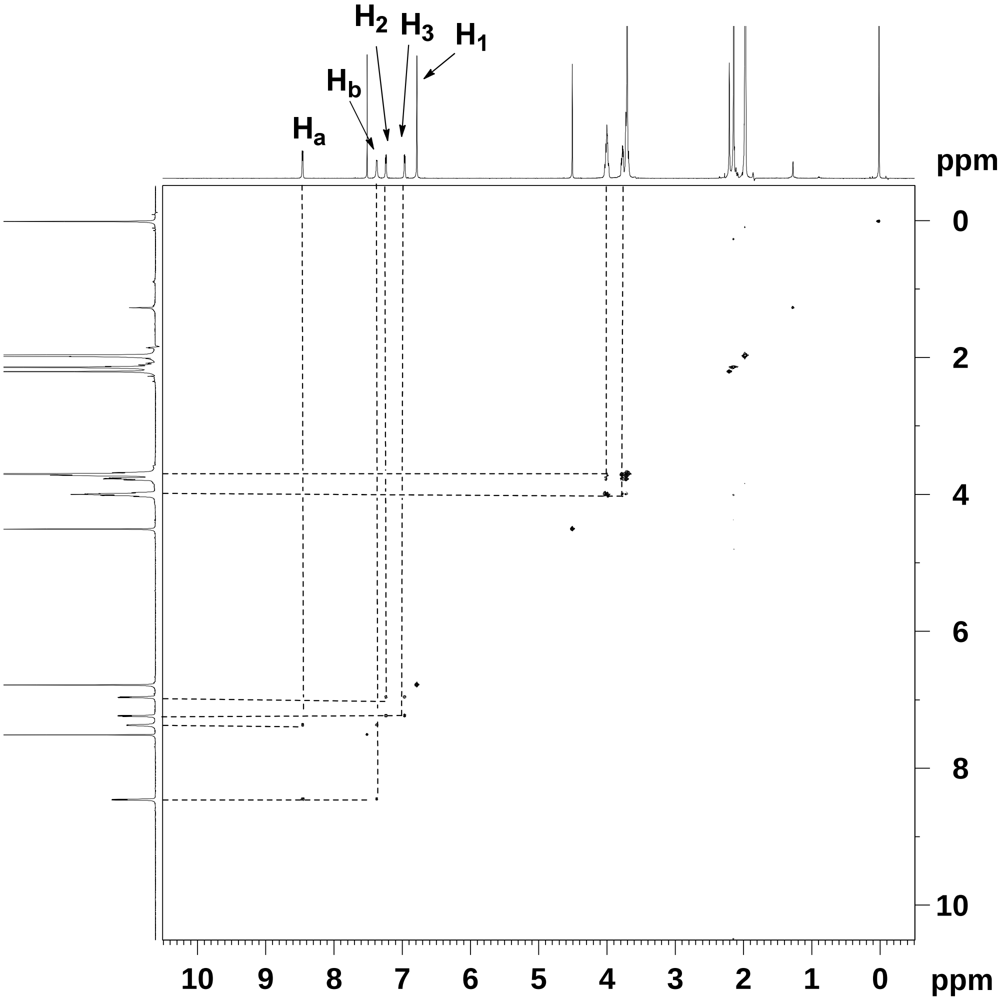

Figure S14. ¹H-¹H COSY spectrum (600 MHz, $CD_3CN/CDCl_3$=1:1, v/v, 298 K) of **1** and 1.0 equiv. of **3**. $[\mathbf{1}]_0$ = 3.0 mM.

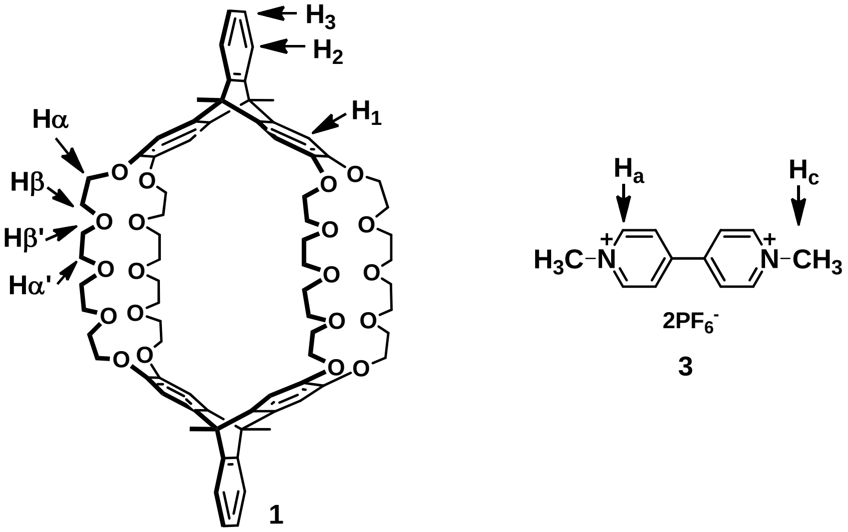

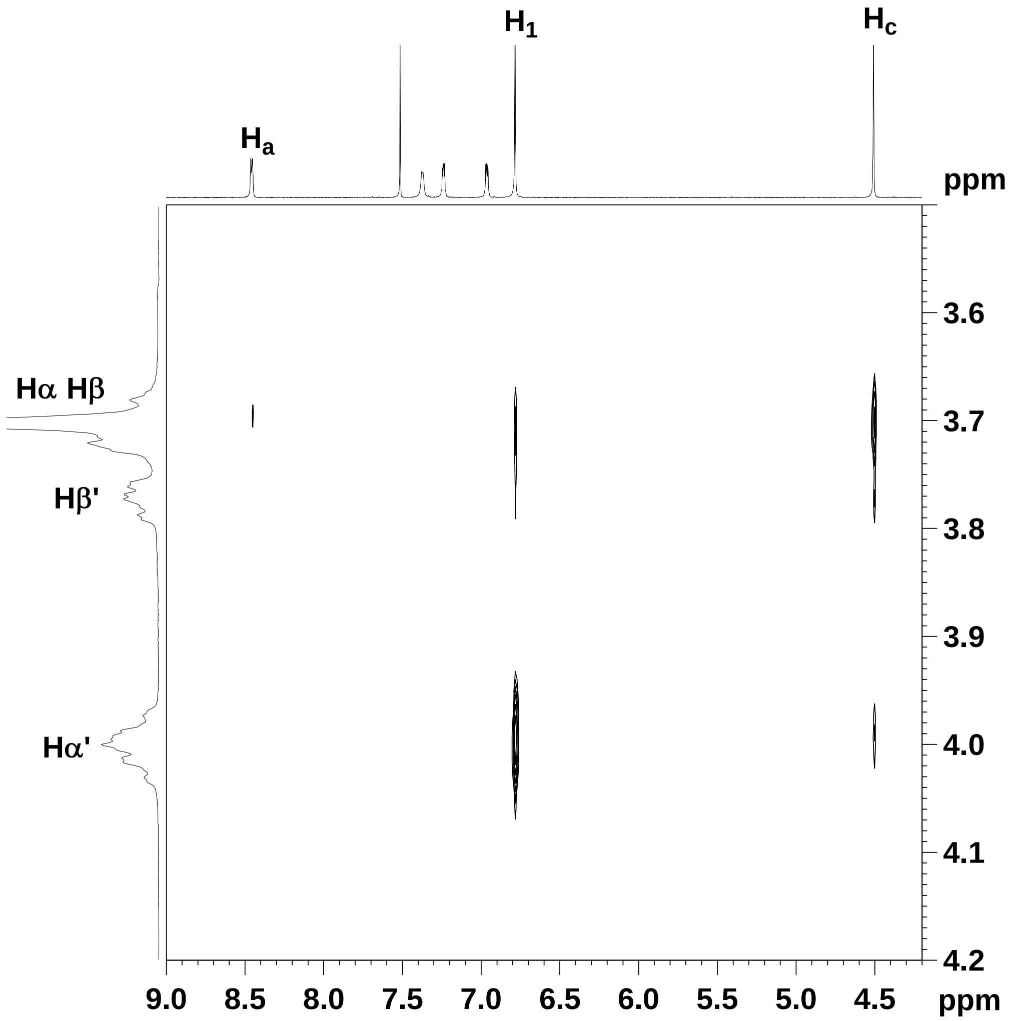

Figure S15. ^{1}H-^{1}H ROESY spectrum (600 MHz, $CD_3CN/CDCl_3$=1:1, v/v, 298 K) of **1** and 1.0 equiv. of **3**. [**1**]$_0$ = 3.0 mM.

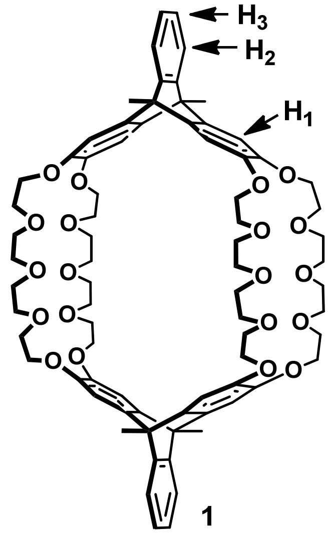

1

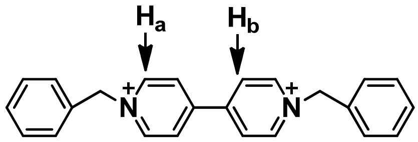

$2PF_6^-$

4

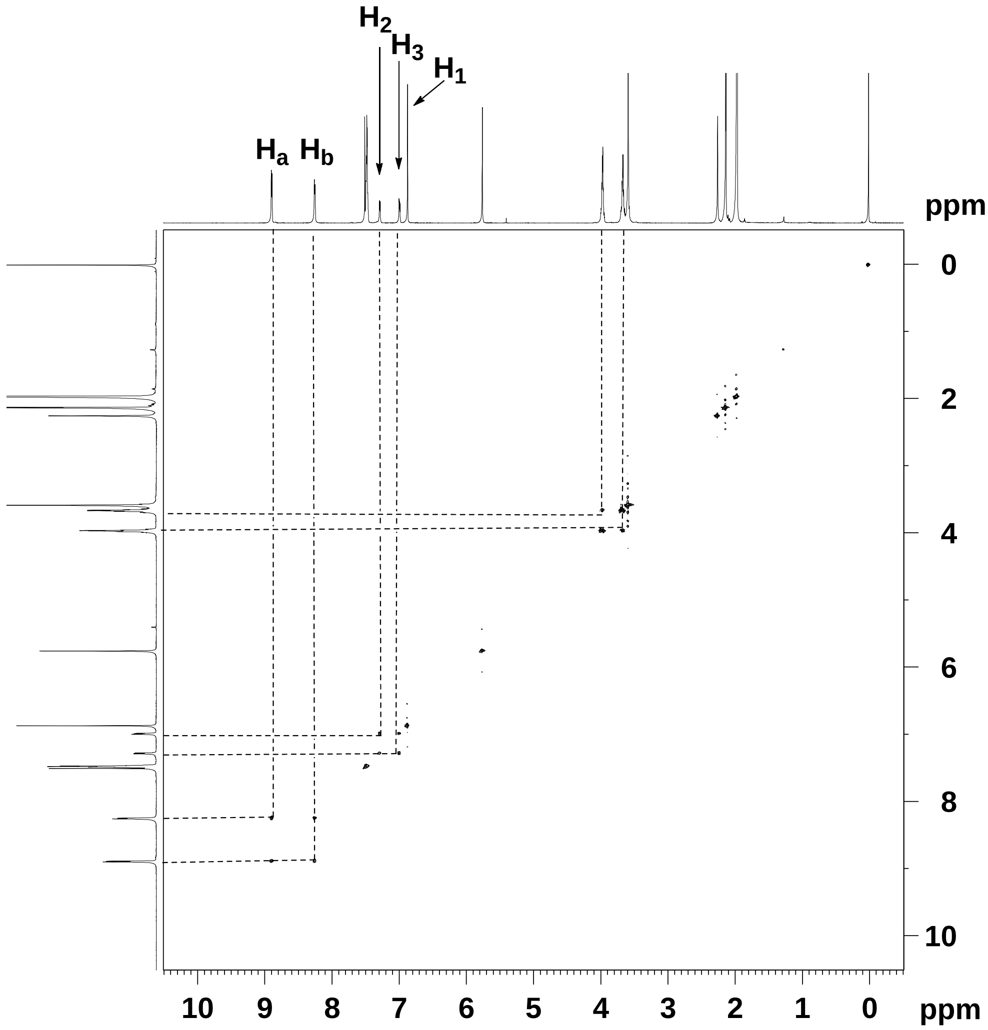

Figure 16. ^{1}H-^{1}H COSY spectrum (600 MHz, $CD_3CN/CDCl_3$=1:1, v/v, 298 K) of **1** and 1.0 equiv. of **4**. [**1**]$_0$ = 3.0 mM.

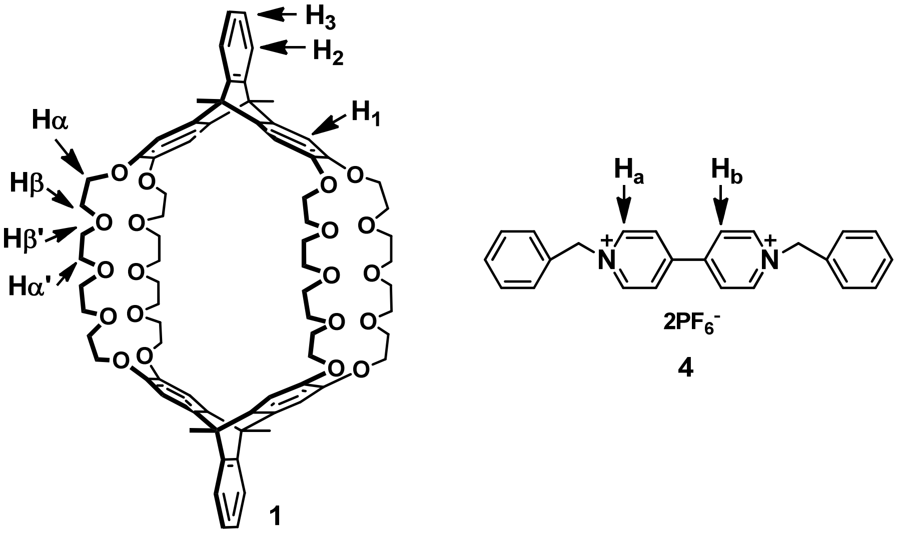

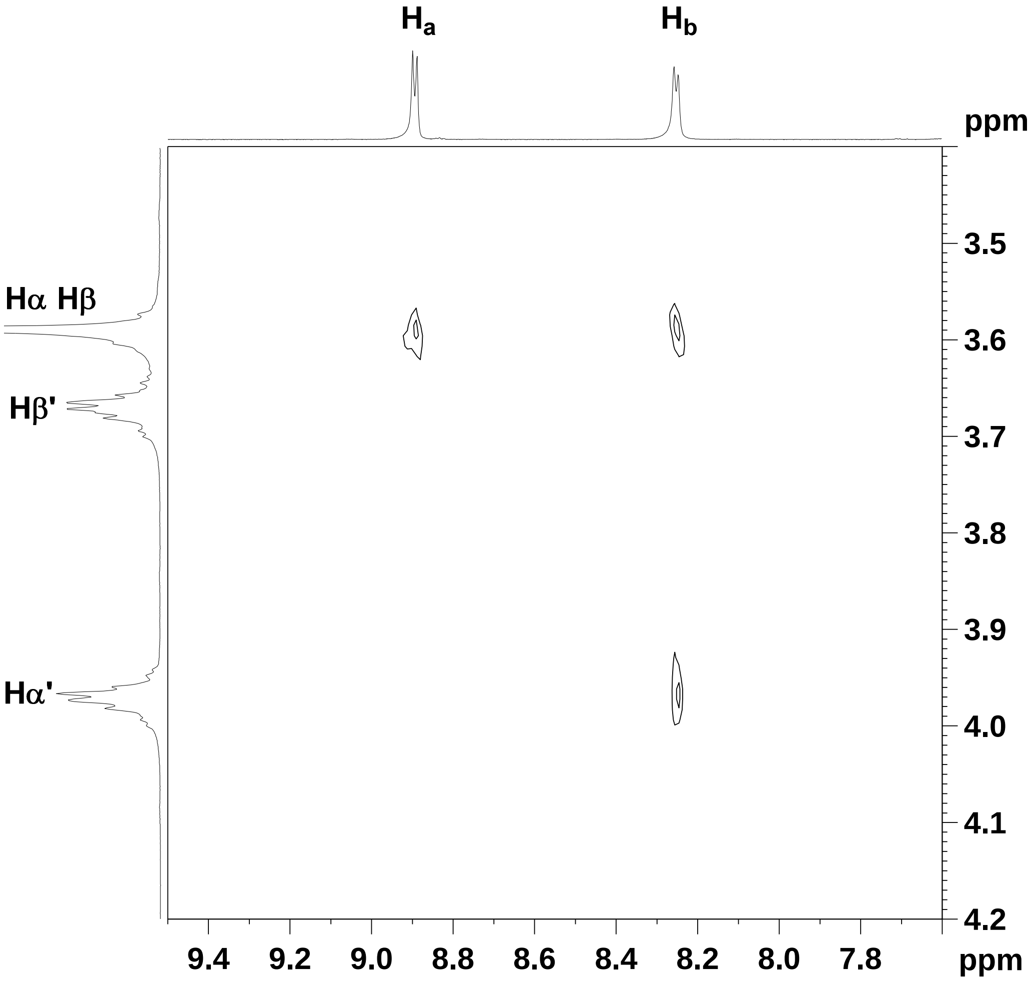

Figure S17. ^{1}H-^{1}H ROESY spectrum (600 MHz, $CD_3CN/CDCl_3$=1:1, v/v, 298 K) of **1** and 1.0 equiv. of **4**. [**1**]$_0$ = 3.0 mM.

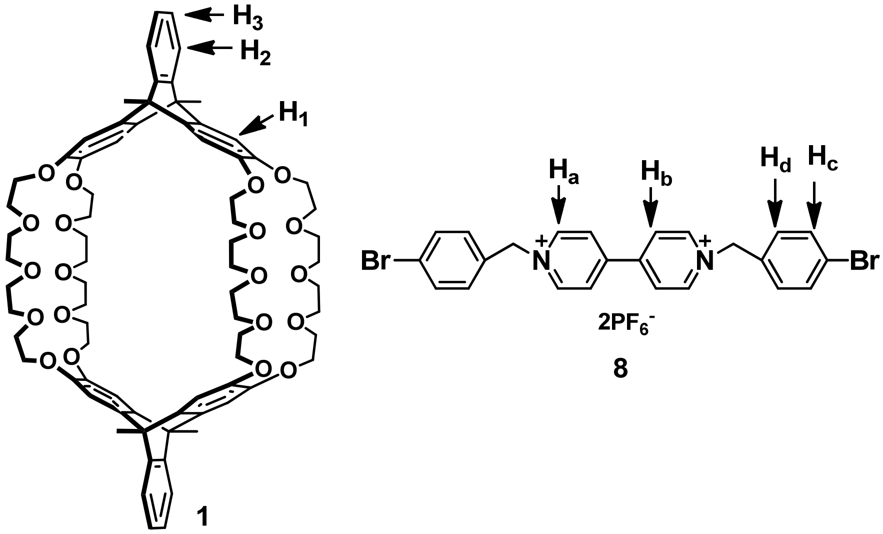

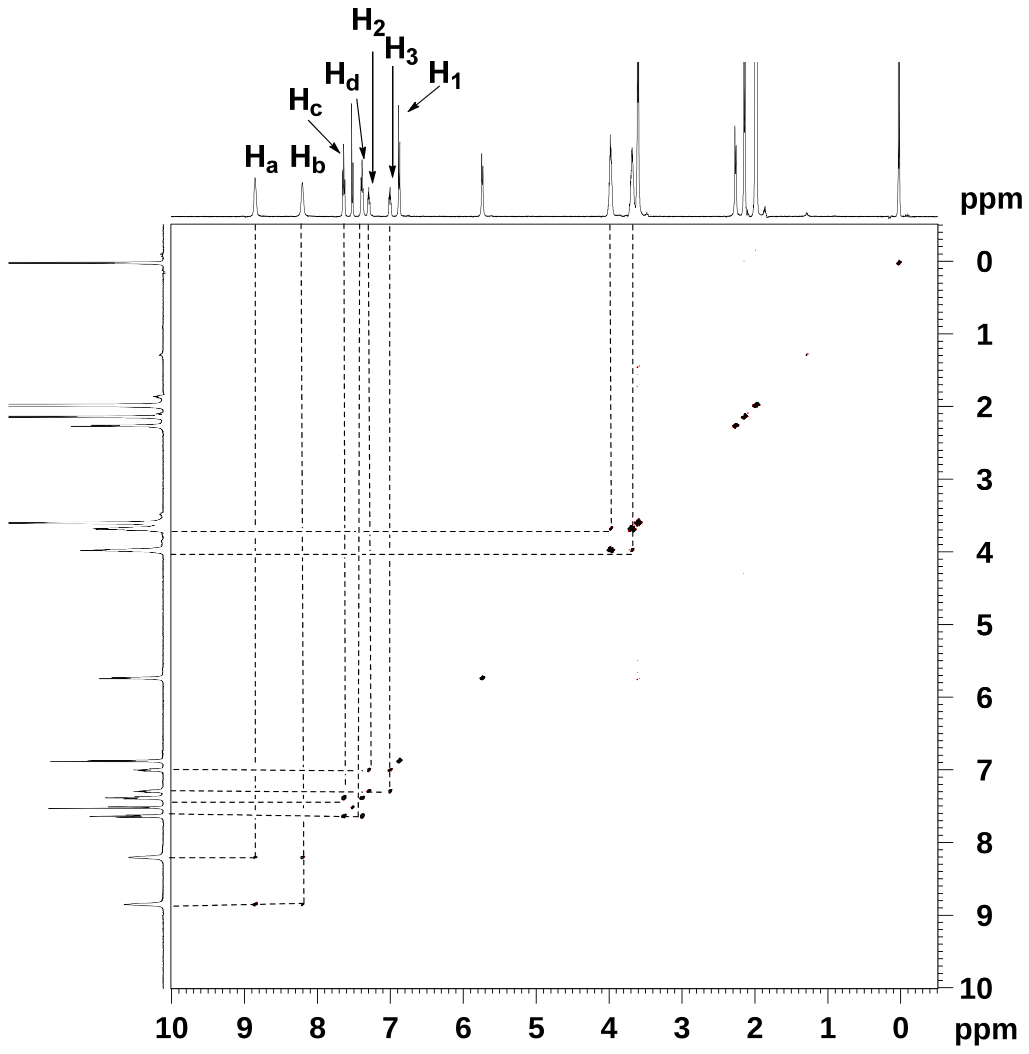

Figure S18. ^{1}H-^{1}H COSY spectrum (600 MHz, $CD_3CN/CDCl_3$=1:1, v/v, 298 K) of **1** and 1.0 equiv. of **8**. [**1**]$_0$ = 3.0 mM.

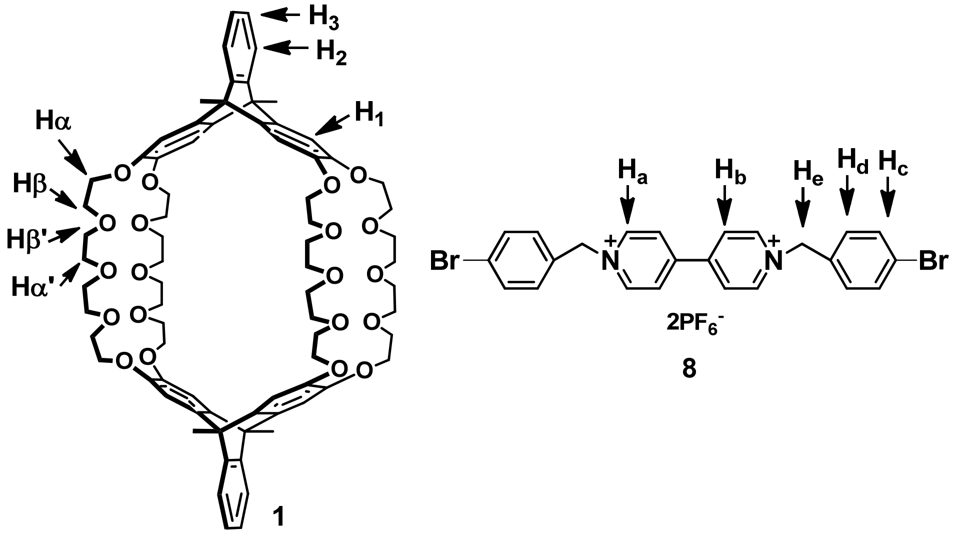

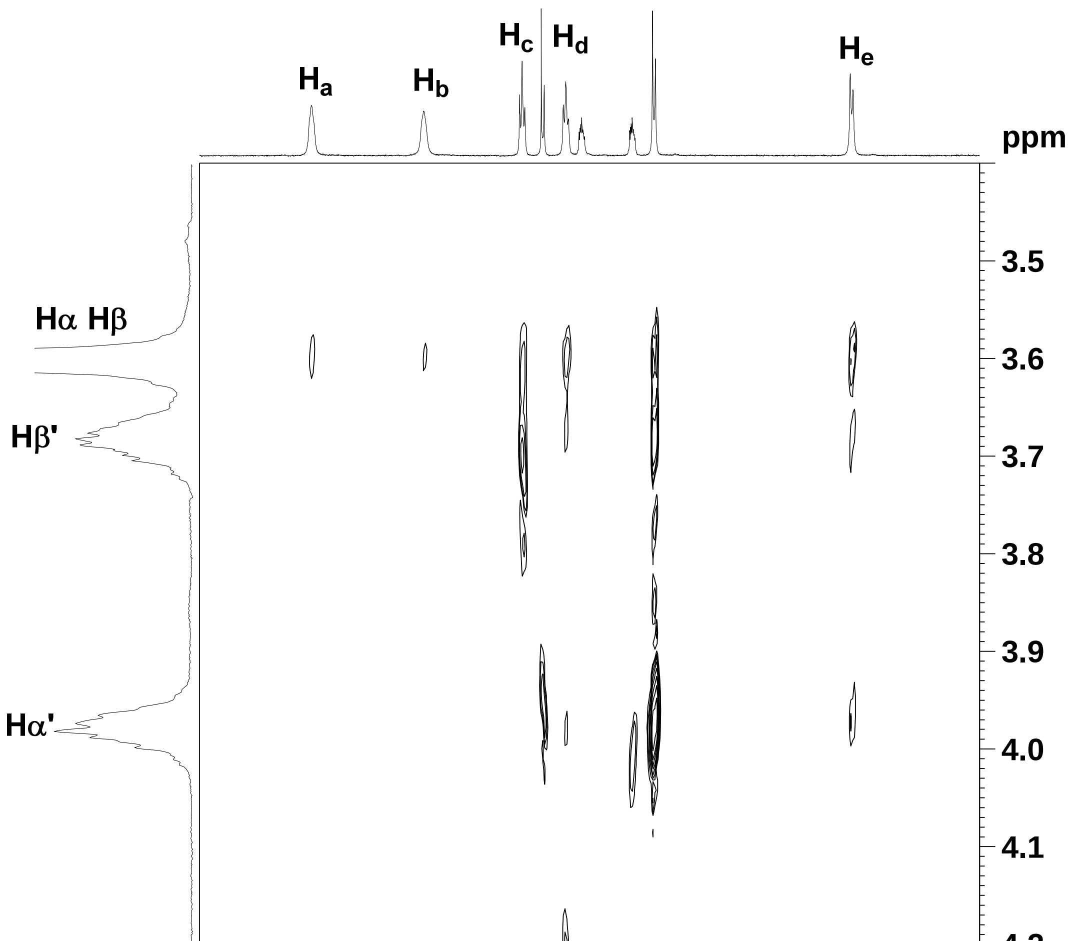

Figure S19. ^{1}H-^{1}H ROESY spectrum (600 MHz, $CD_3CN/CDCl_3$=1:1, v/v, 298 K) of **1** and 1.0 equiv. of **8**. [**1**]$_0$ = 3.0 mM.

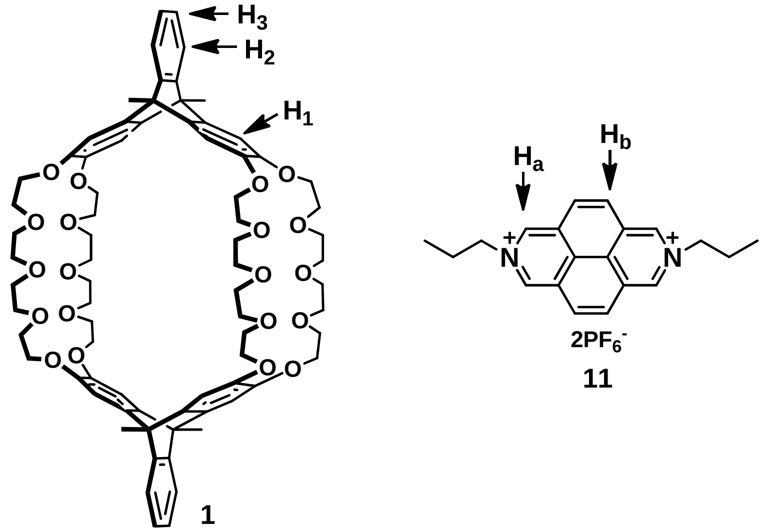

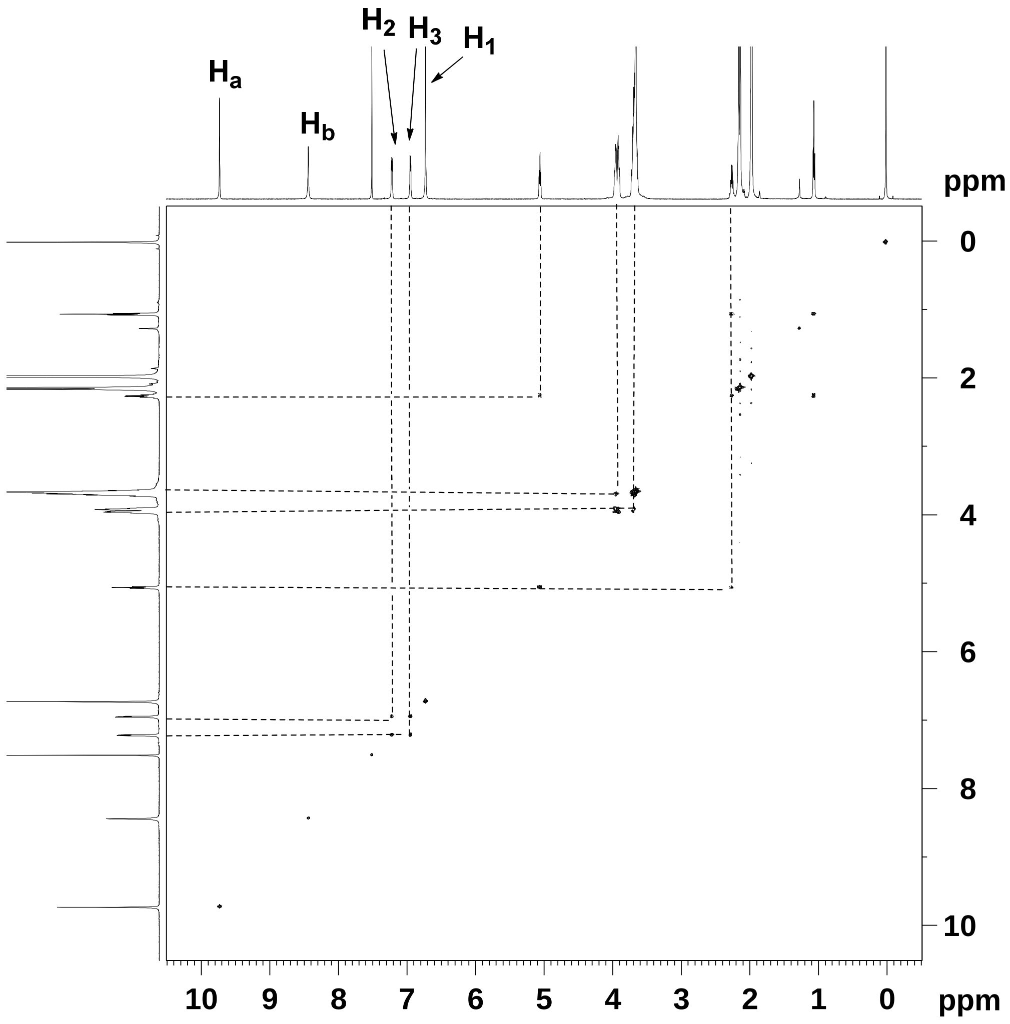

Figure S20. ^{1}H-^{1}H COSY spectrum (600 MHz, $CD_3CN/CDCl_3$=1:1, v/v, 298 K) of **1** and 1.0 equiv. of **11**. $[\mathbf{1}]_0$ = 3.0 mM.

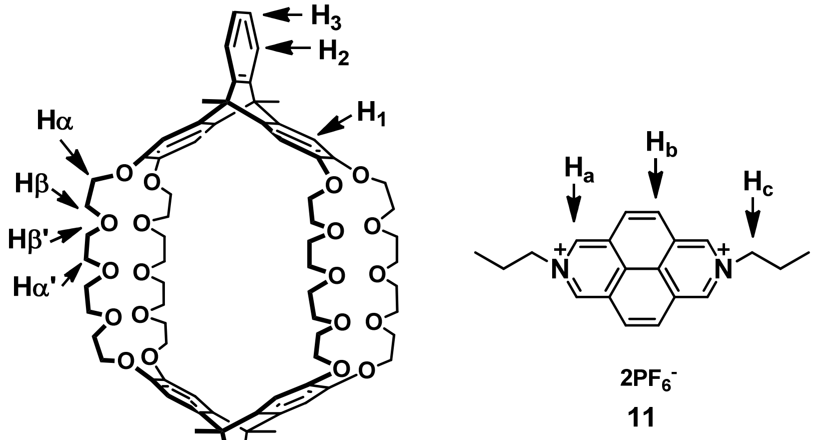

1

2PF6-

11

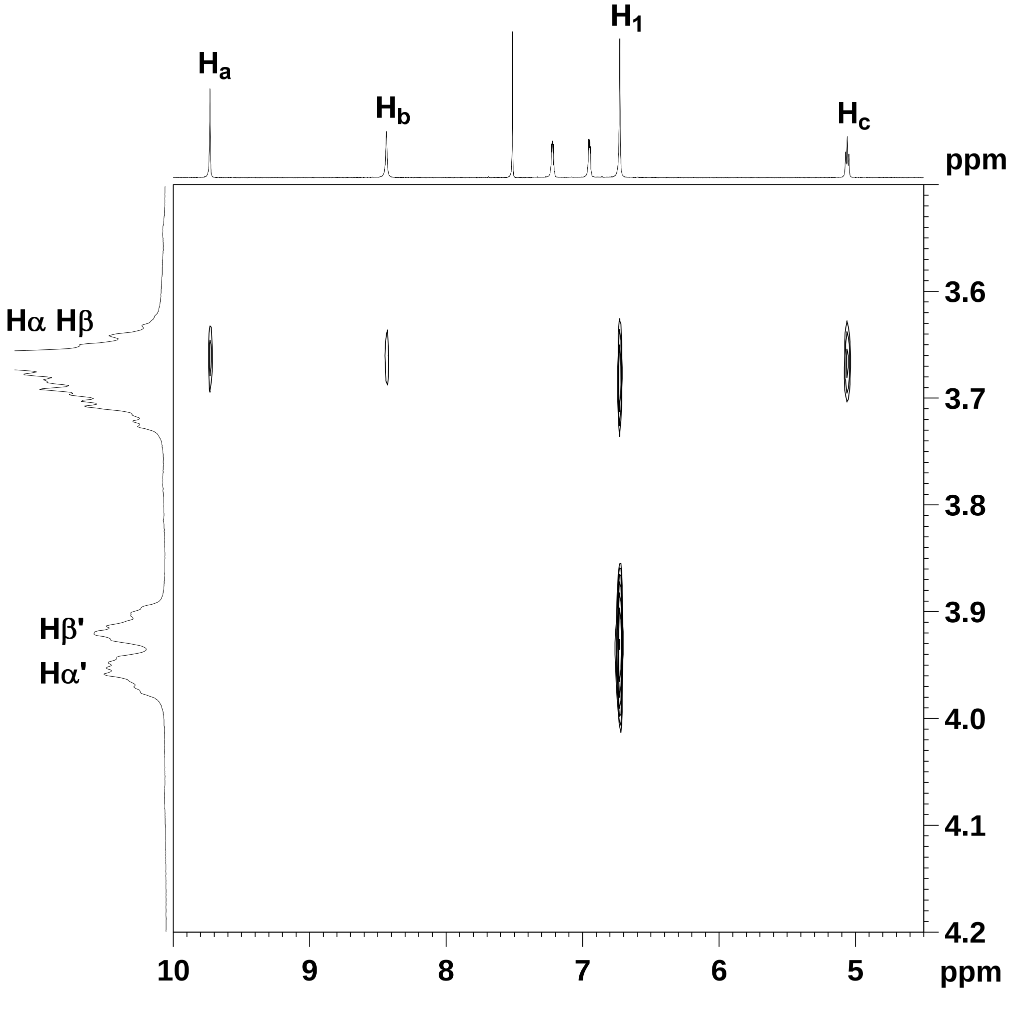

Figure S21. ^1H-^1H ROESY spectrum (600 MHz, $CD_3CN/CDCl_3$=1:1, v/v, 298 K) of **1** and 1.0 equiv. of **11**. [**1**]$_0$ = 3.0 mM.

4. Determination of the association constants

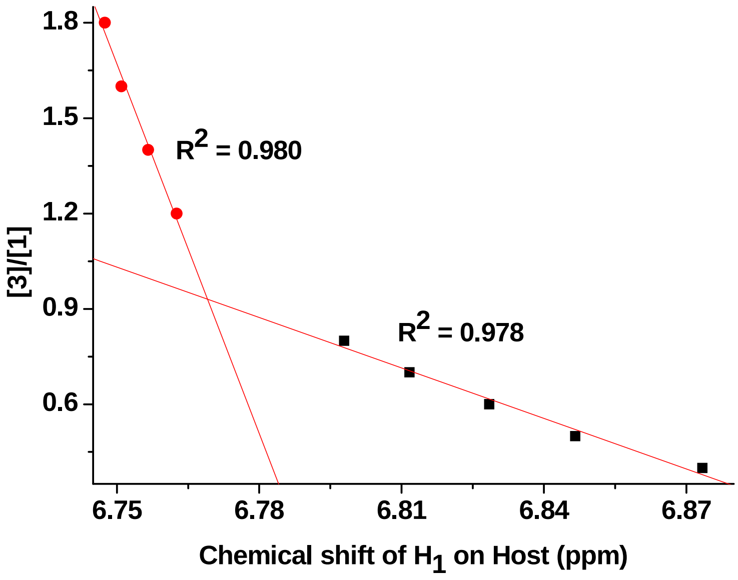

Figure S22. Mole ratio plot for the complexation of **1** and **3** in $CD_3CN/CDCl_3$ = 1:1 at 298 K.

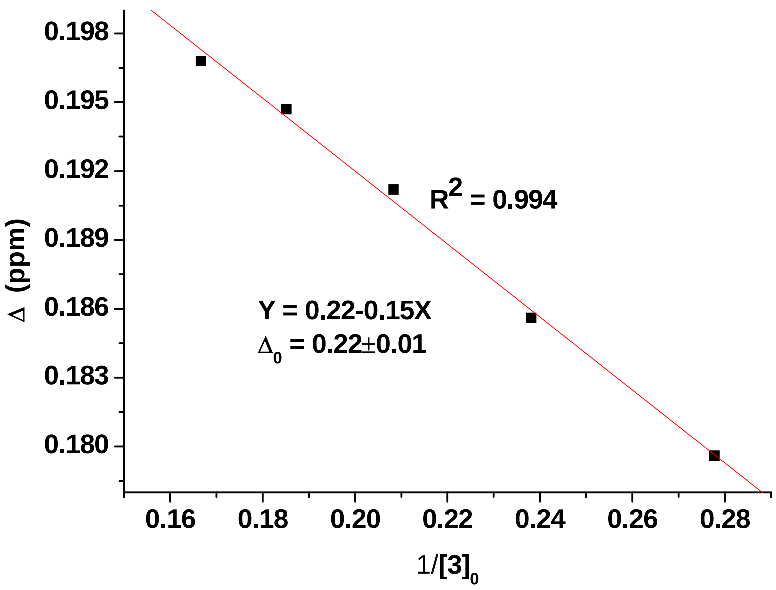

Figure S23. Determination of Δ_0 of H_1 for the complexation of **1** and **3** in $CD_3CN/CDCl_3$ = 1:1 at 298 K.

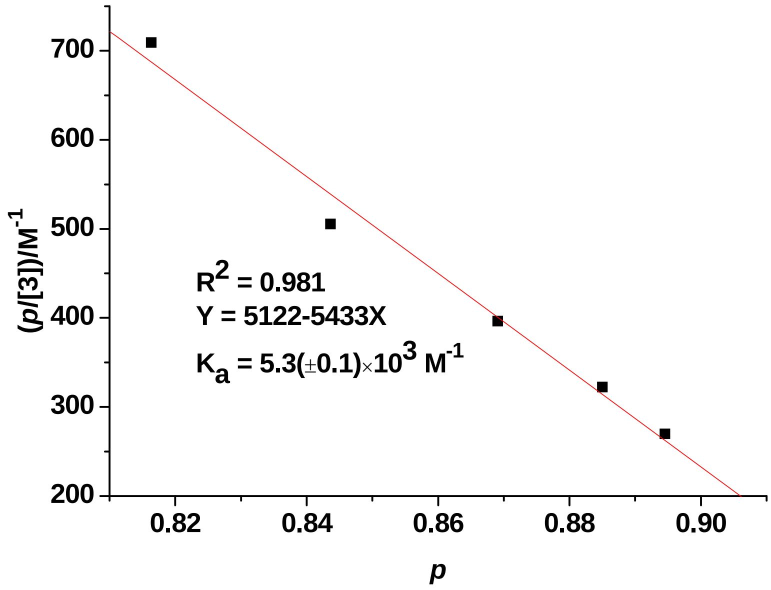

Figure S24. Scatchard plot for the complexation of **1** and **3** in $CD_3CN/CDCl_3$ = 1:1 at 298 K.

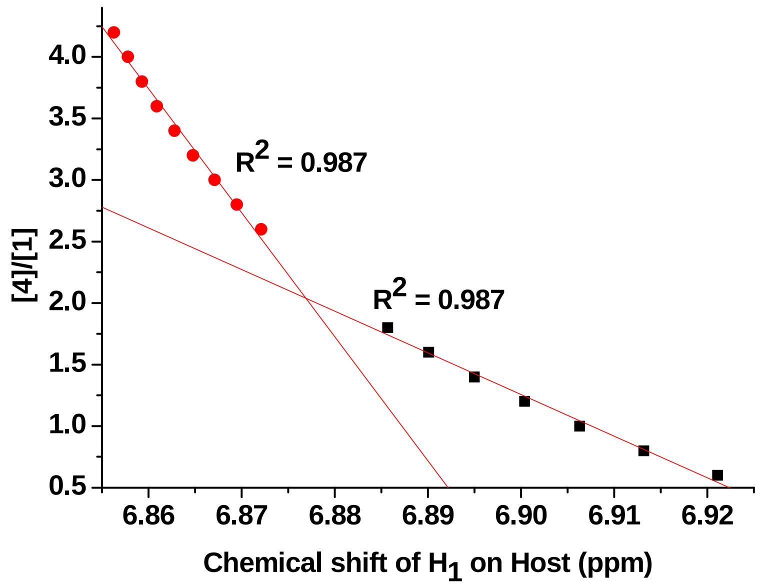

Figure S25. Mole ratio plot for the complexation of **1** and **4** in $CD_3CN/CDCl_3$ = 1:1 at 298 K.

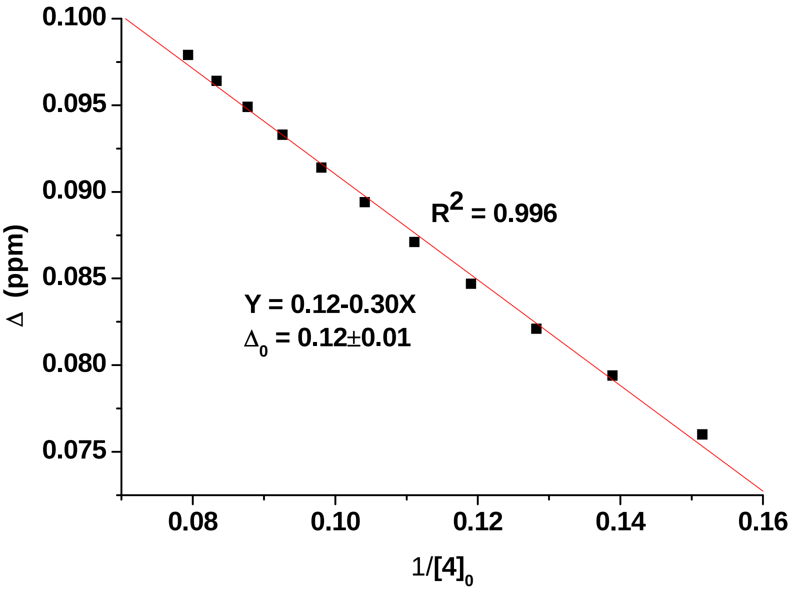

Figure S26. Determination of Δ_0 of H_1 for the complexation of **1** and **4** in $CD_3CN/CDCl_3$ = 1:1 at 298 K.

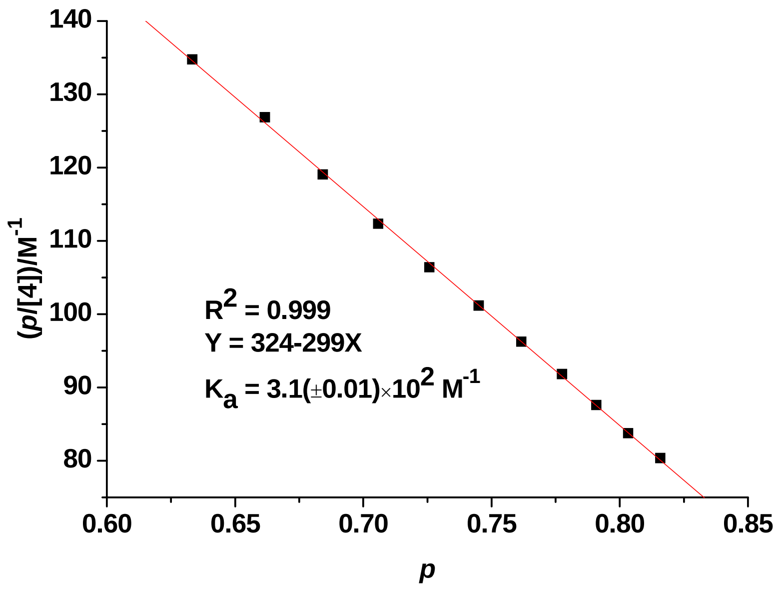

Figure S27. Scatchard plot for the complexation of **1** and **4** in $CD_3CN/CDCl_3$ = 1:1 at 298 K.

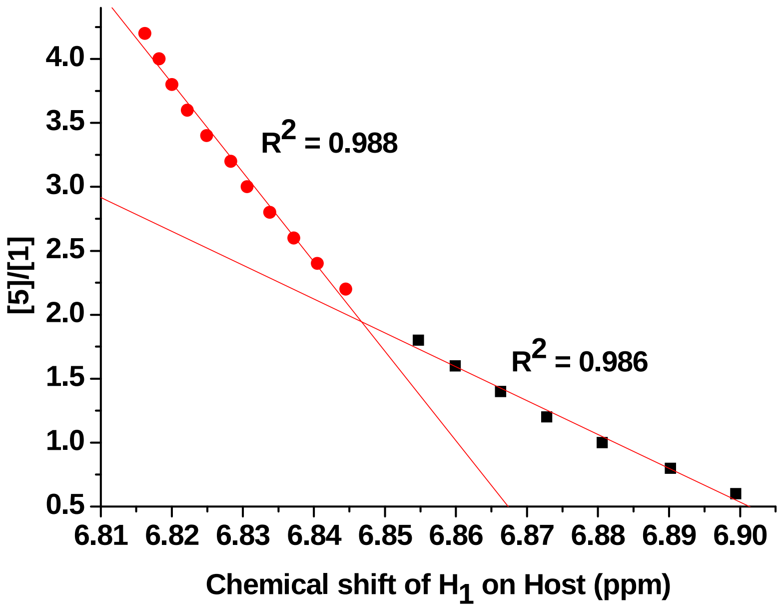

Figure S28. Mole ratio plot for the complexation of **1** and **5** in $CD_3CN/CDCl_3 = 1:1$ at 298 K.

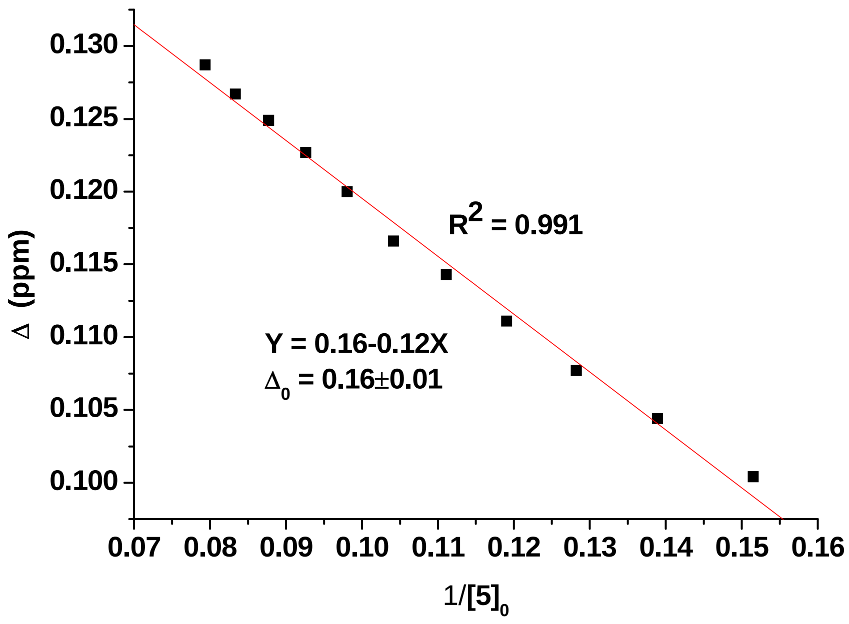

Figure S29. Determination of Δ_0 of H_1 for the complexation of **1** and **5** in $CD_3CN/CDCl_3 = 1:1$ at 298 K.

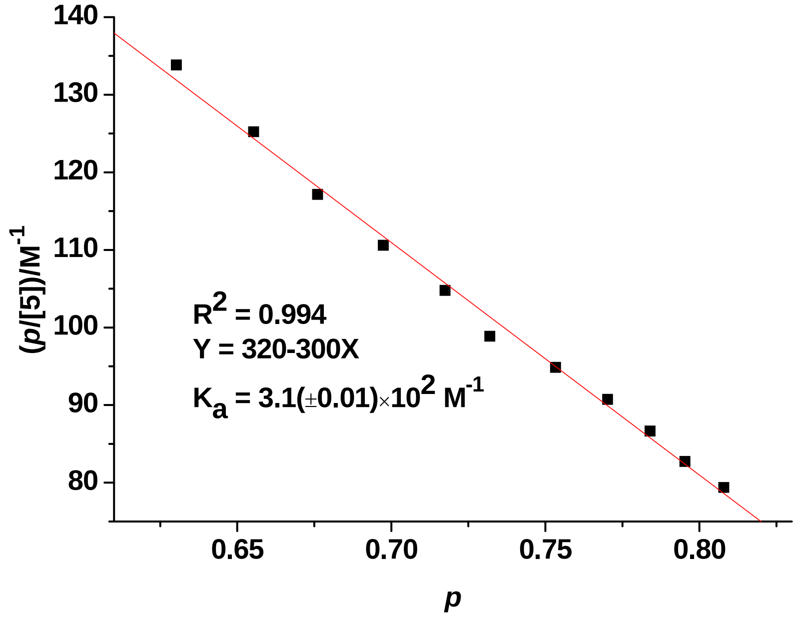

Figure S30. Scatchard plot for the complexation of **1** and **5** in $CD_3CN/CDCl_3$ = 1:1 at 298 K.

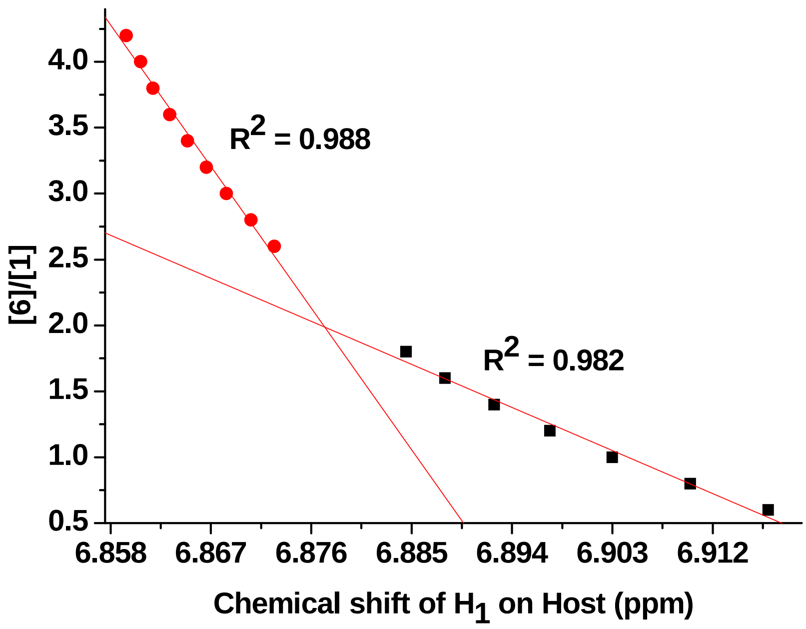

Figure S31. Mole ratio plot for the complexation of **1** and **6** in $CD_3CN/CDCl_3$ = 1:1 at 298 K.

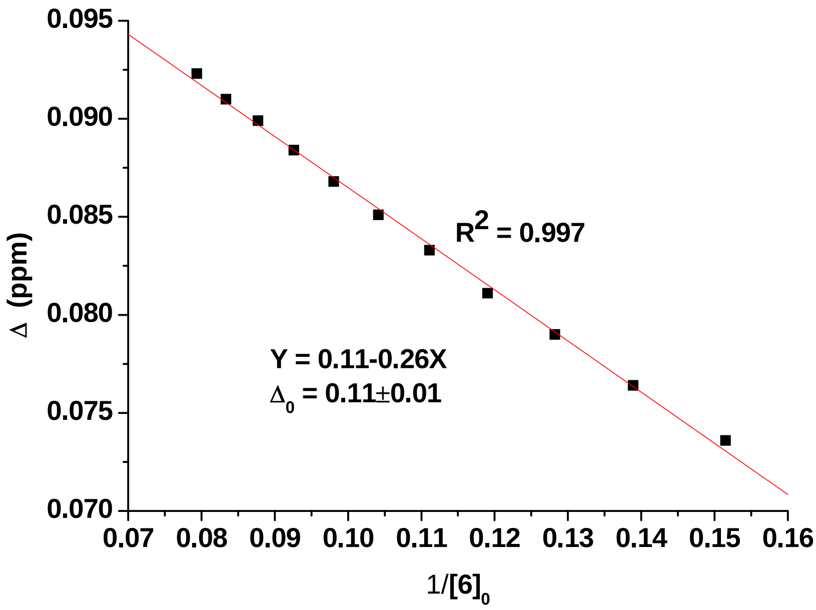

Figure S32. Determination of Δ_0 of H_1 for the complexation of **1** and **6** in $CD_3CN/CDCl_3 = 1:1$ at 298 K.

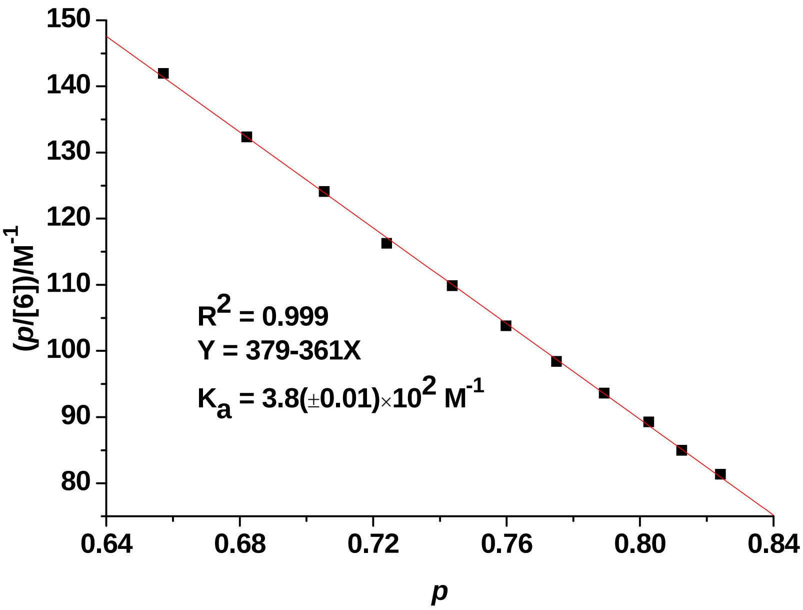

Figure S33. Scatchard plot for the complexation of **1** and **6** in $CD_3CN/CDCl_3 = 1:1$ at 298 K.

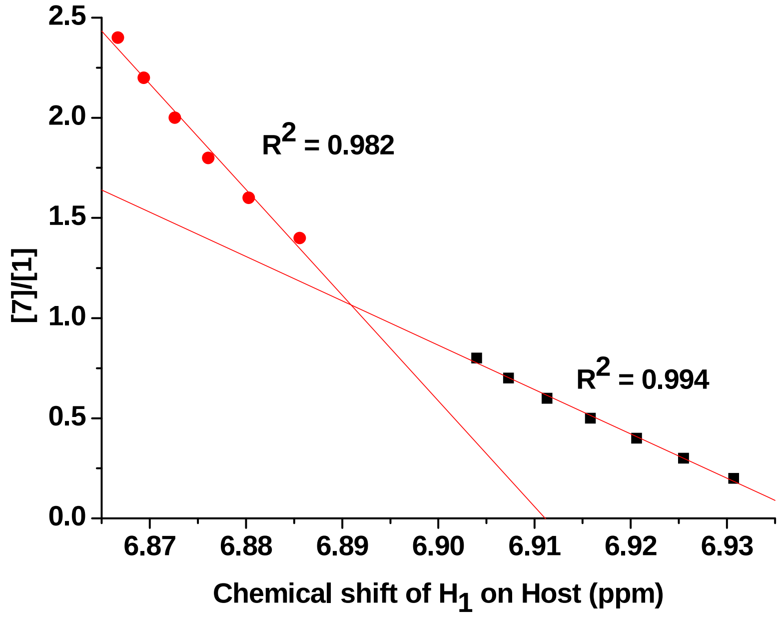

Figure S34. Mole ratio plot for the complexation of **1** and **7** in $CD_3CN/CDCl_3$ = 1:1 at 298 K.

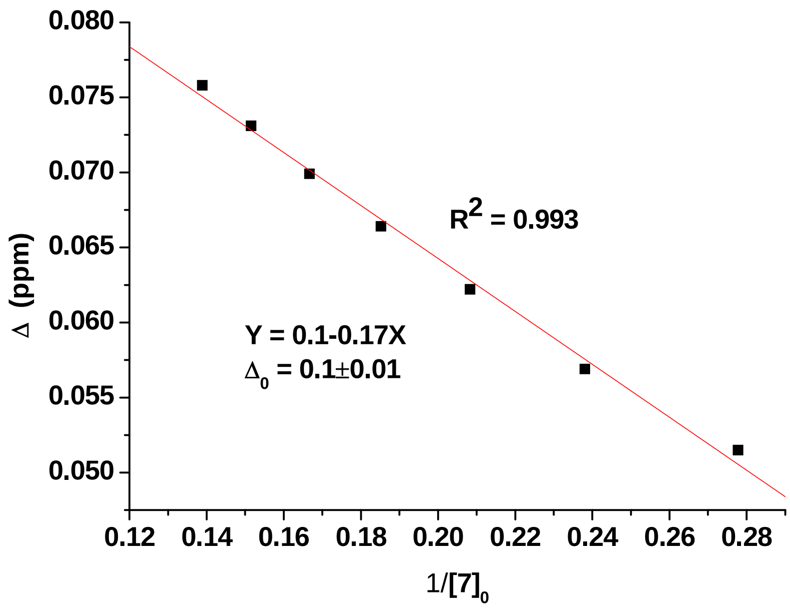

Figure S35. Determination of Δ_0 of H_1 for the complexation of **1** and **7** in $CD_3CN/CDCl_3$ = 1:1 at 298 K.

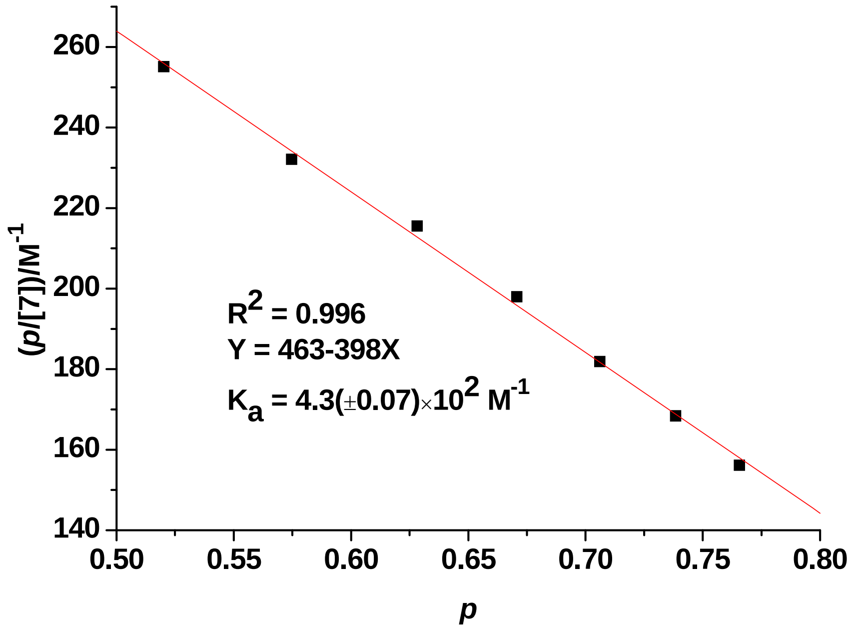

Figure S36. Scatchard plot for the complexation of **1** and **7** in $CD_3CN/CDCl_3 = 1{:}1$ at 298 K.

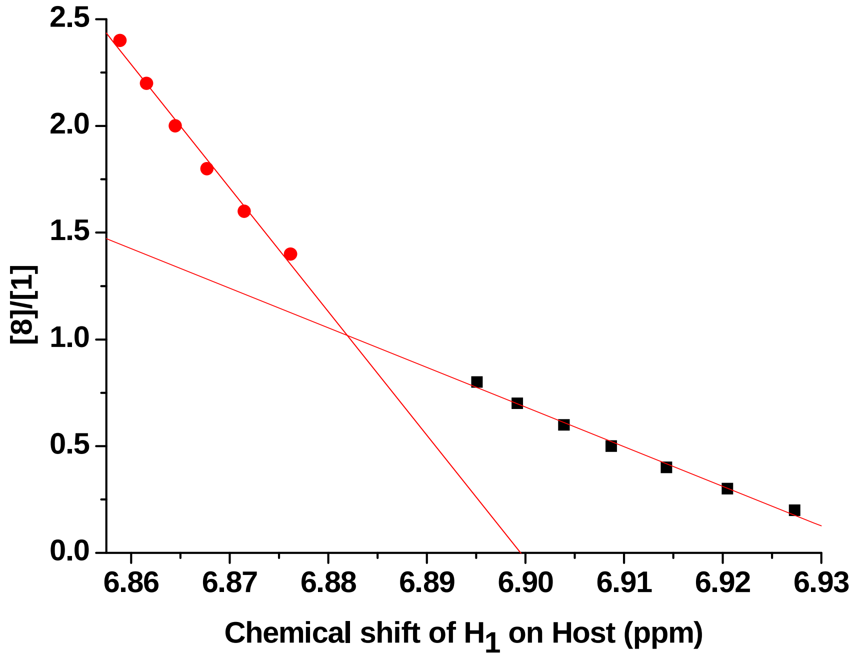

Figure S37. Mole ratio plot for the complexation of **1** and **8** in $CD_3CN/CDCl_3 = 1{:}1$ at 298 K.

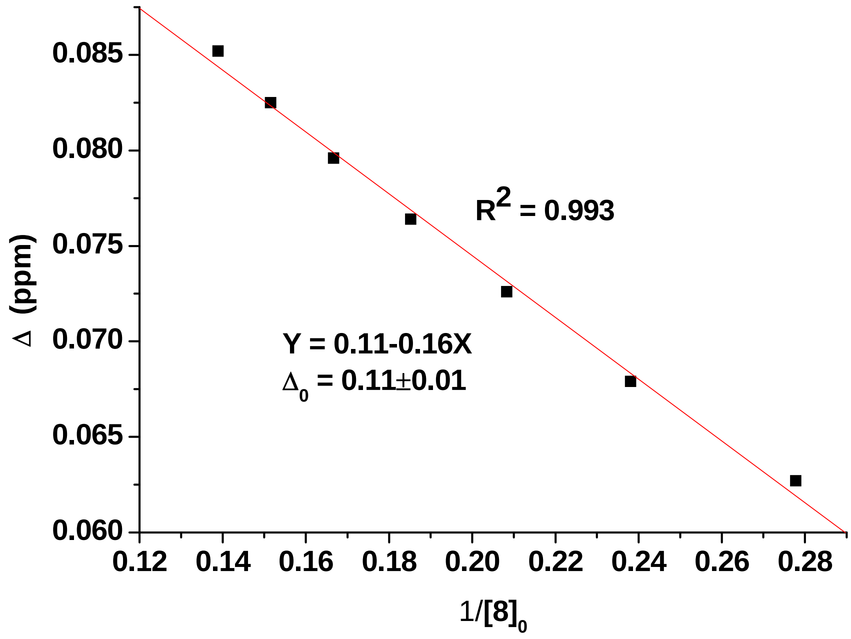

Figure S38. Determination of Δ_0 of H_1 for the complexation of **1** and **8** in $CD_3CN/CDCl_3$ = 1:1 at 298 K.

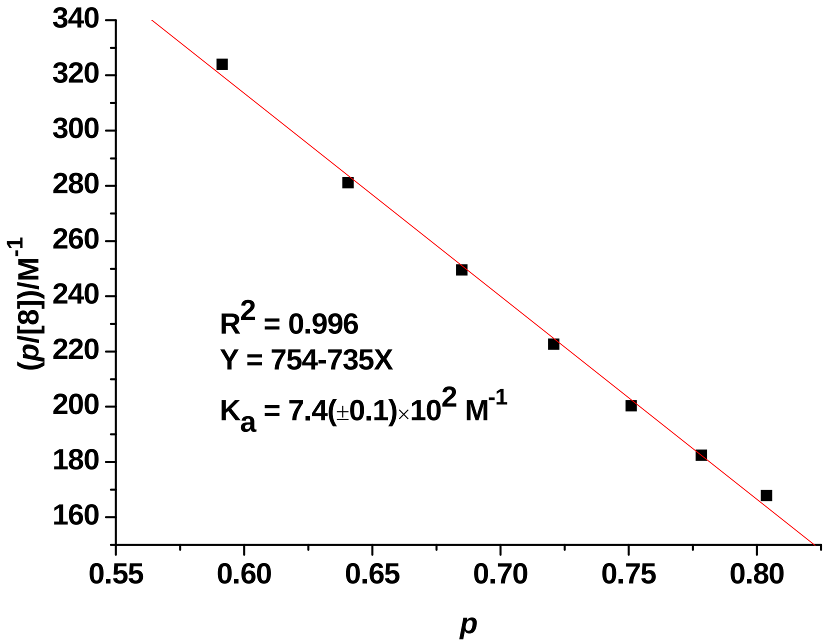

Figure S39. Scatchard plot for the complexation of **1** and **8** in $CD_3CN/CDCl_3$ = 1:1 at 298 K.

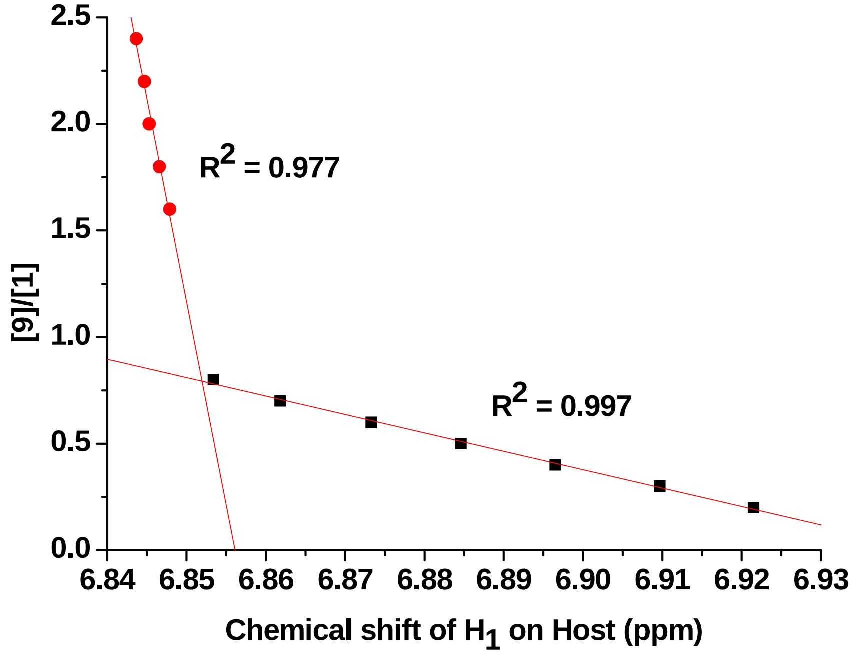

Figure S40. Mole ratio plot for the complexation of **1** and **9** in $CD_3CN/CDCl_3 = 1:1$ at 298 K.

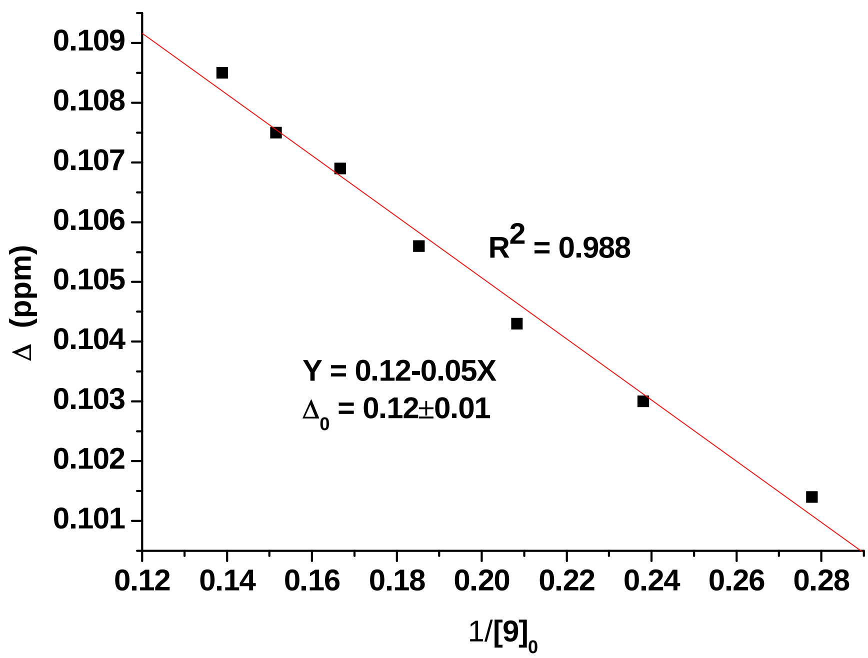

Figure S41. Determination of Δ_0 of H_1 for the complexation of **1** and **9** in $CD_3CN/CDCl_3 = 1:1$ at 298 K.

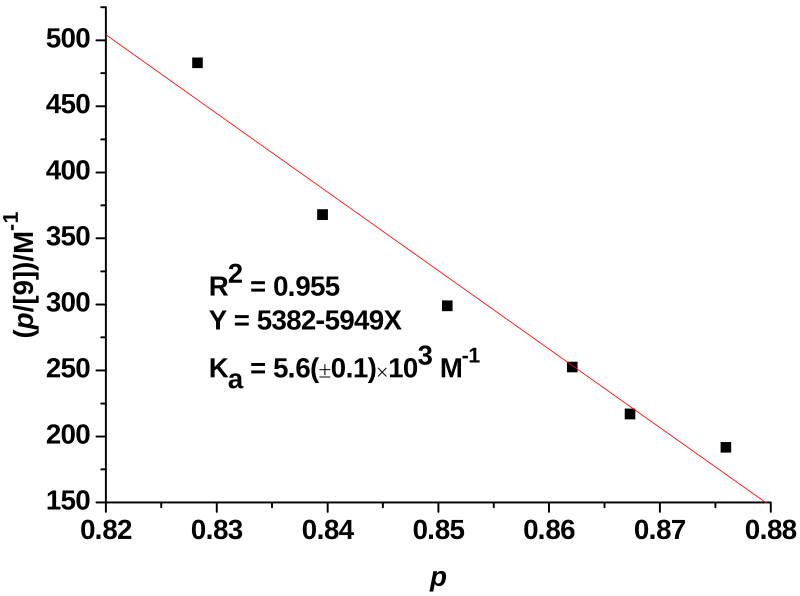

Figure S42. Scatchard plot for the complexation of **1** and **9** in $CD_3CN/CDCl_3 = 1:1$ at 298 K.

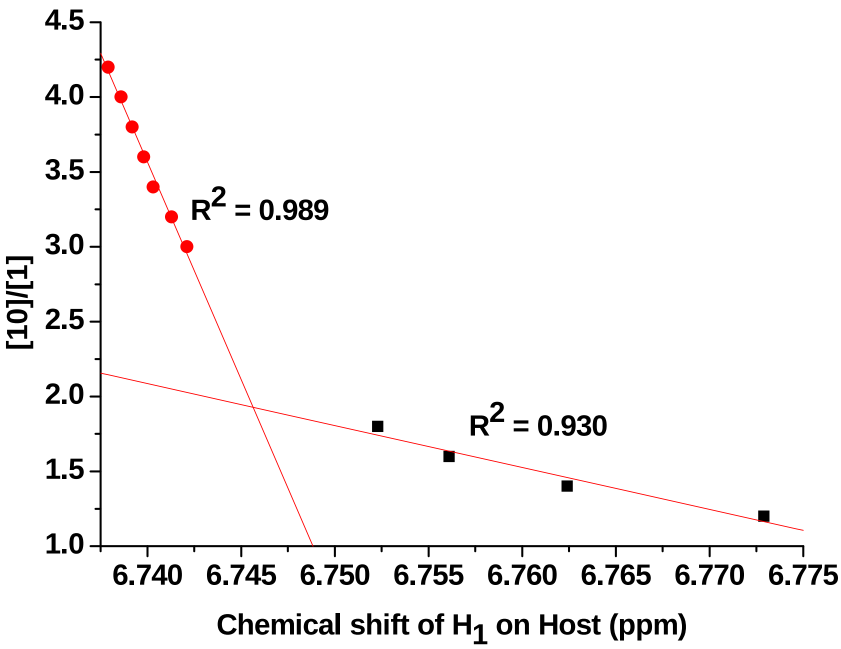

Figure S43. Mole ratio plot for the complexation of **1** and **10** in $CD_3CN/CDCl_3 = 1:1$ at 298 K.

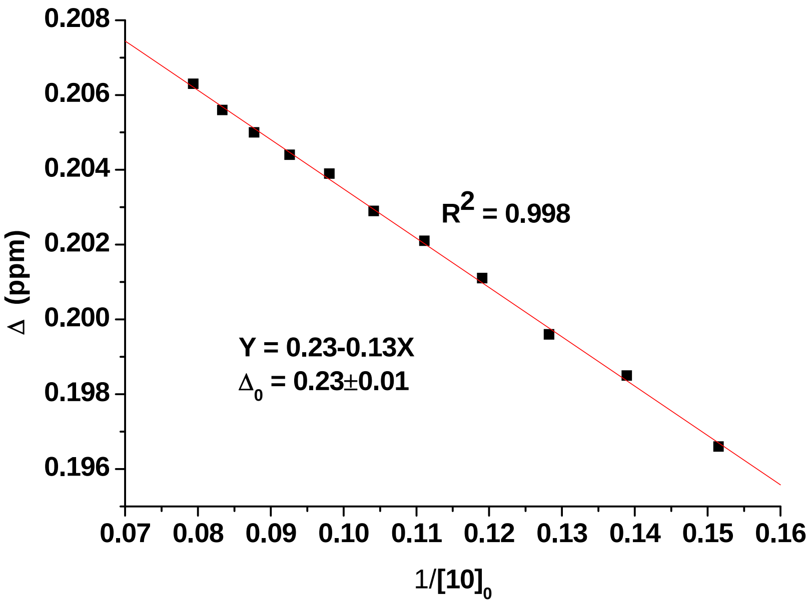

Figure S44. Determination of Δ_0 of H_1 for the complexation of **1** and **10** in $CD_3CN/CDCl_3$ = 1:1 (v/v) at 298 K.

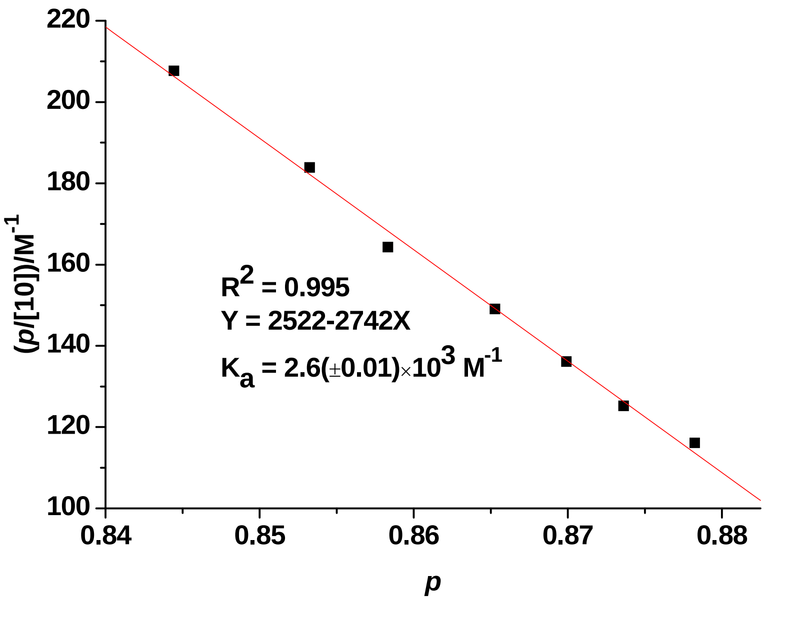

Figure S45. Scatchard plot for the complexation of **1** and **10** in $CD_3CN/CDCl_3$ = 1:1 at 298 K.

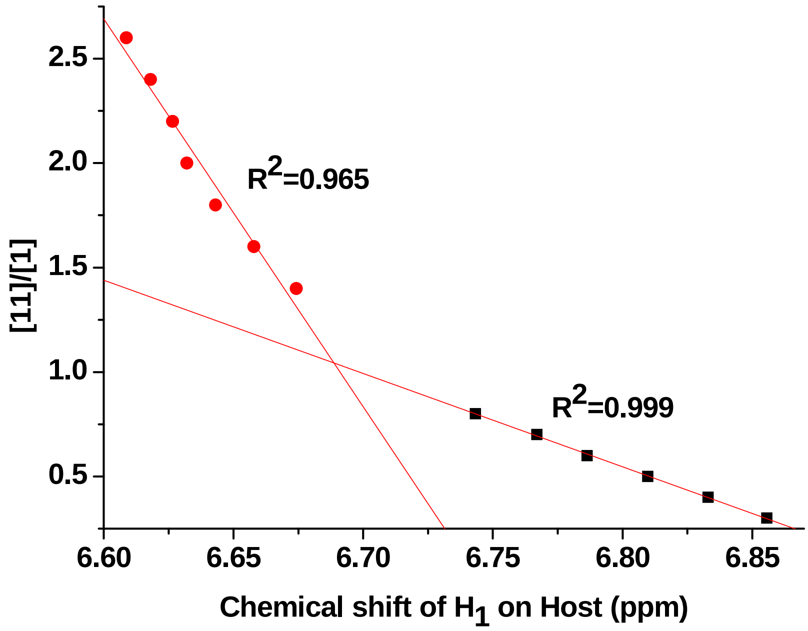

Figure S46. Mole ratio plot for the complexation of **1** and **11** in $CD_3CN/CDCl_3 = 1:1$ at 298 K.

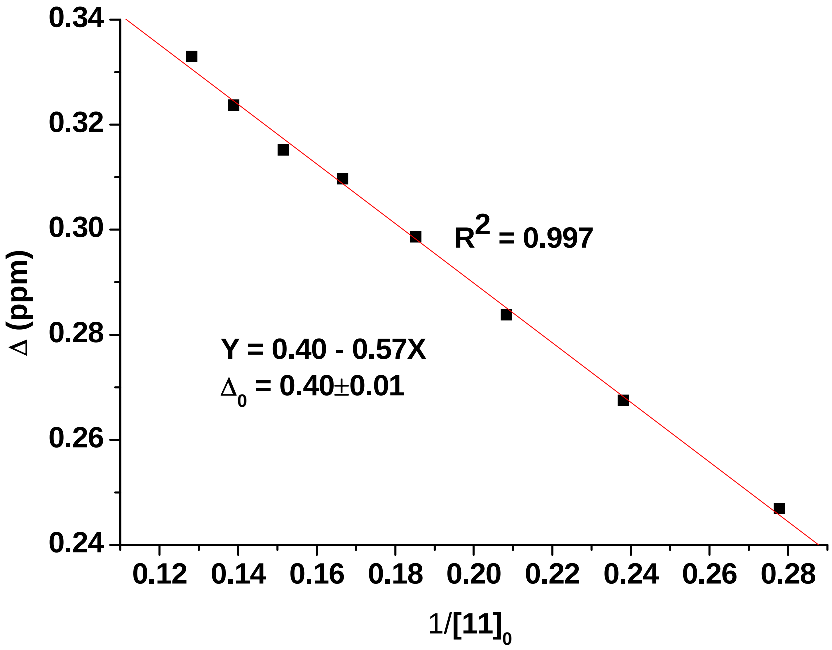

Figure S47. Determination of Δ_0 of H_1 for the complexation of **1** and **11** in $CD_3CN/CDCl_3 = 1:1$ (v/v) at 298 K.

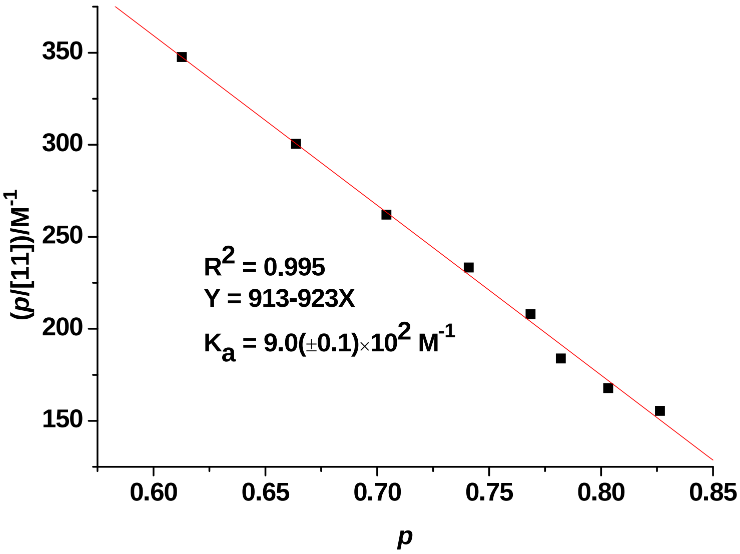

Figure S48. Scatchard plot for the complexation of **1** and **11** in $CD_3CN/CDCl_3$ = 1:1 at 298 K.

5. ESI MS spectra of the complexes

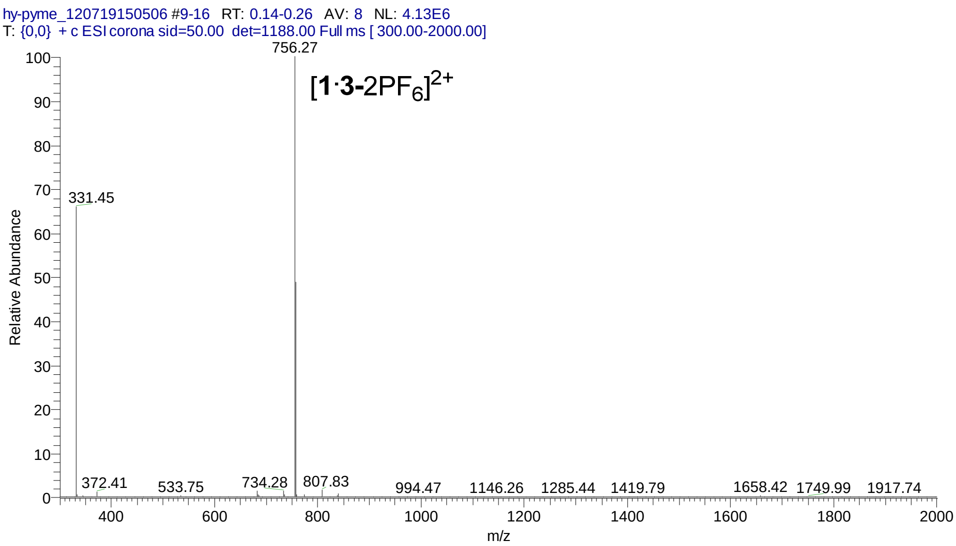

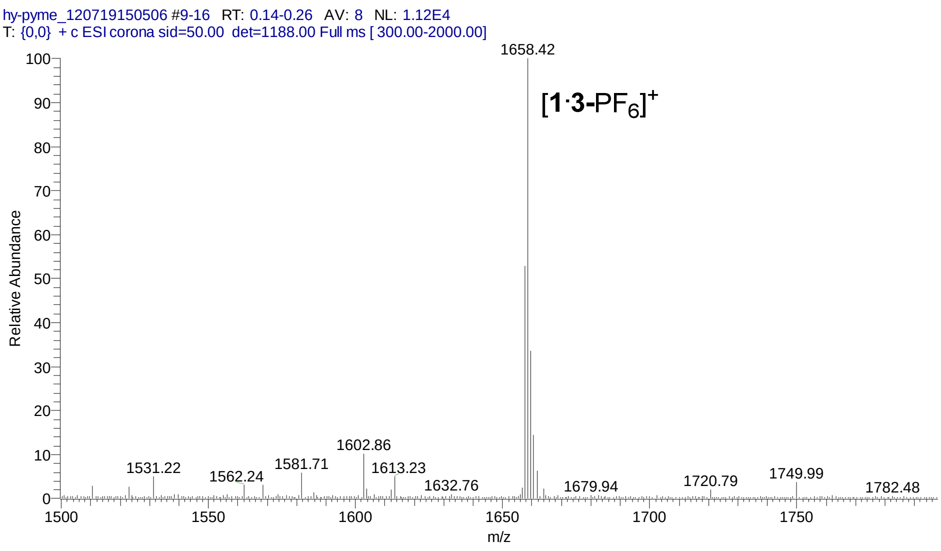

Figure S49. ESI MS of **1** and **3** in acetonitrile-chloroform (1:1, v:v).

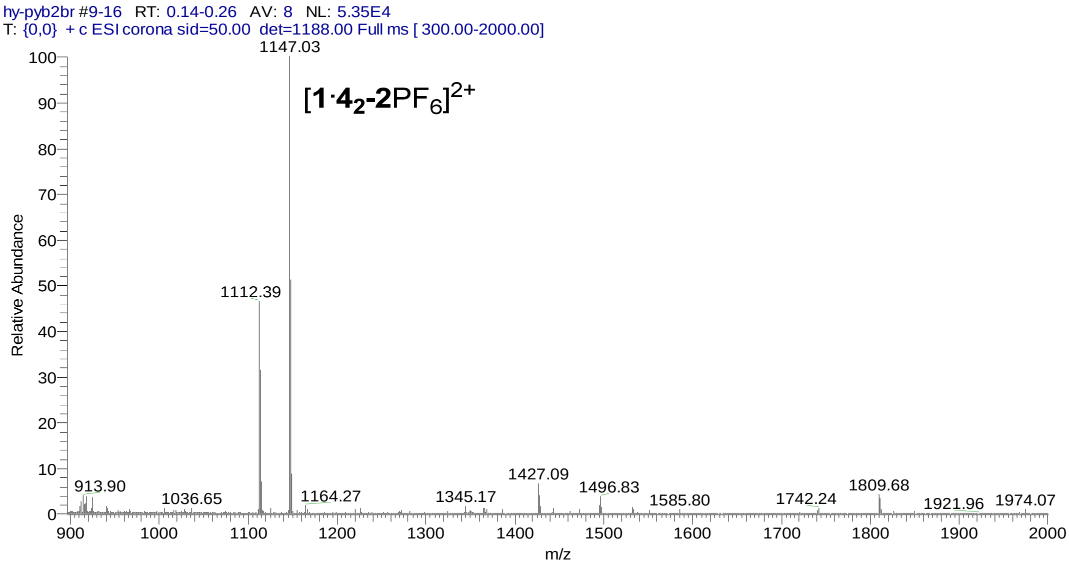

Figure S50. ESI MS of **1** and **4** in acetonitrile-chloroform (1:1, v:v).

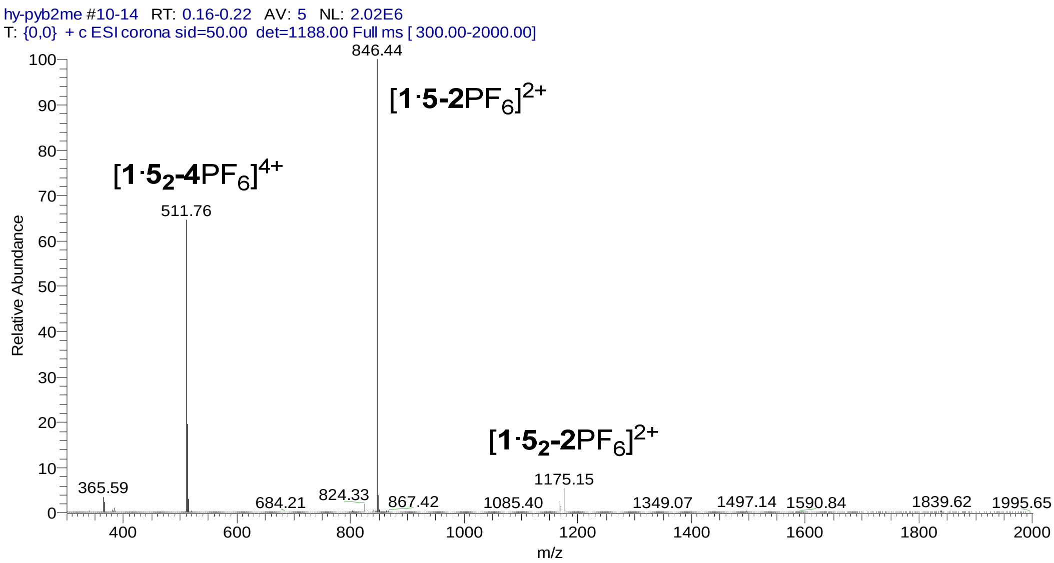

Figure S51. ESI MS of **1** and **5** in acetonitrile-chloroform (1:1, v:v).

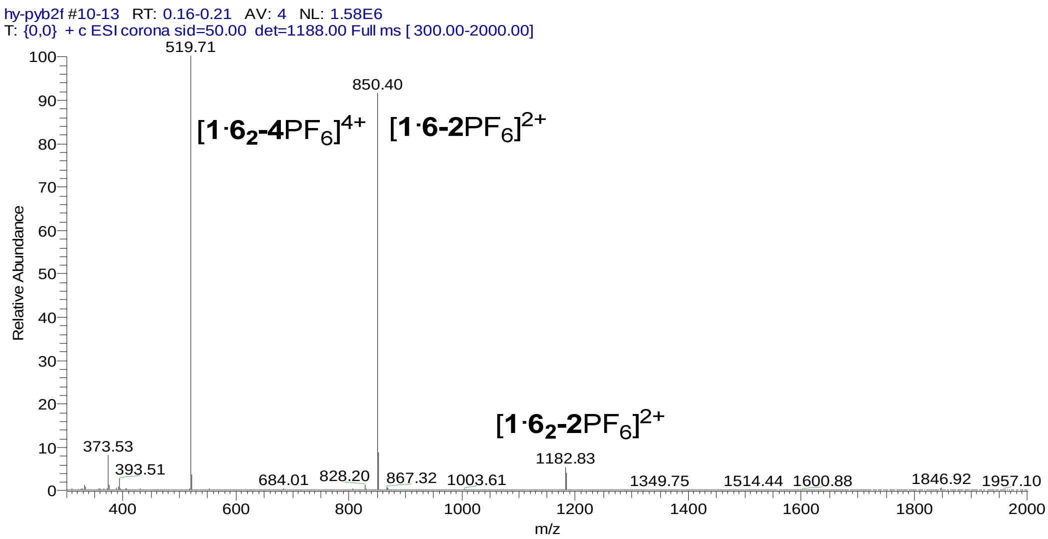

Figure S52. ESI MS of **1** and **6** in acetonitrile-chloroform (1:1, v:v).

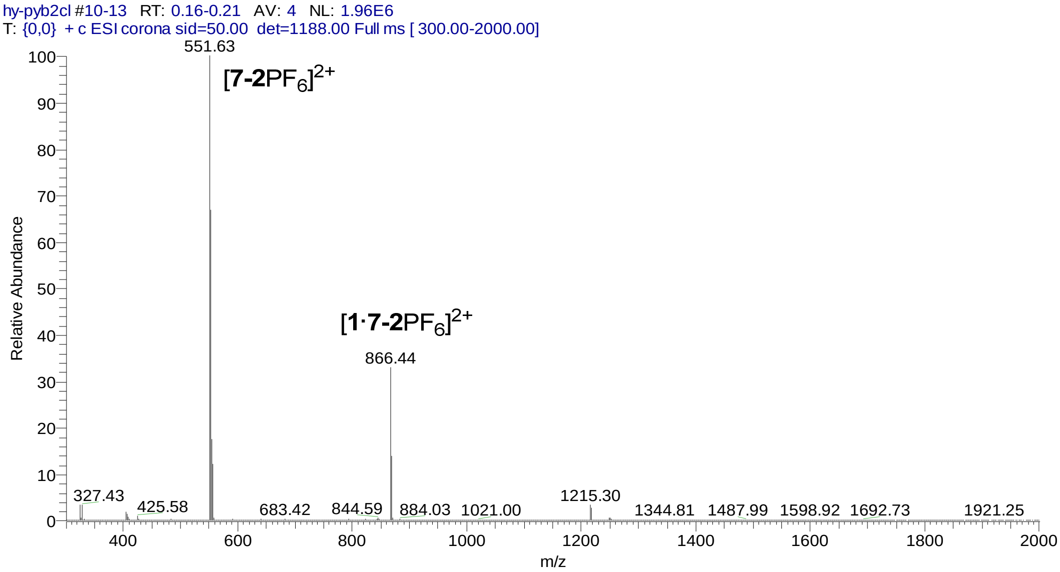

Figure S53. ESI MS of **1** and **7** in acetonitrile-chloroform (1:1, v:v).

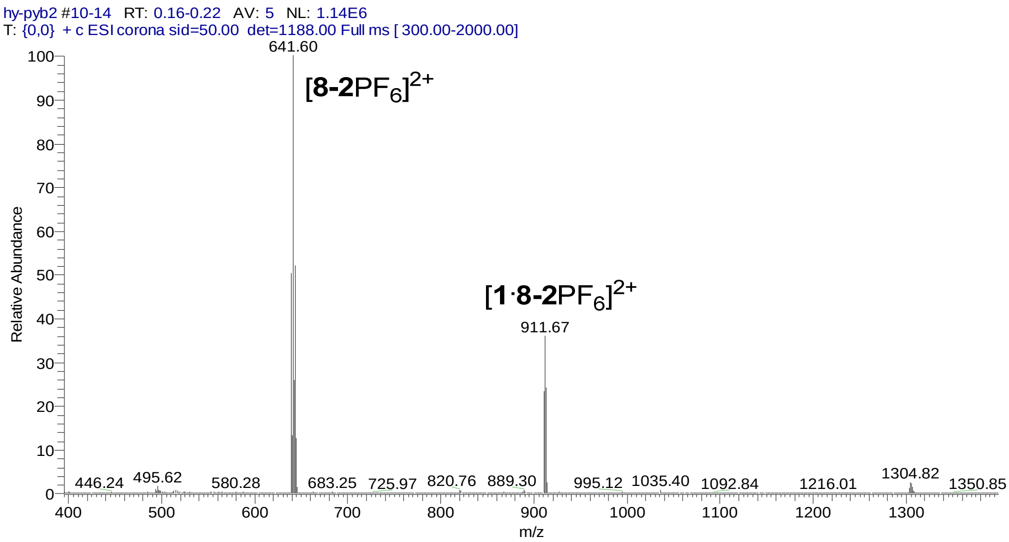

Figure S54. ESI MS of **1** and **8** in acetonitrile-chloroform (1:1, v:v).

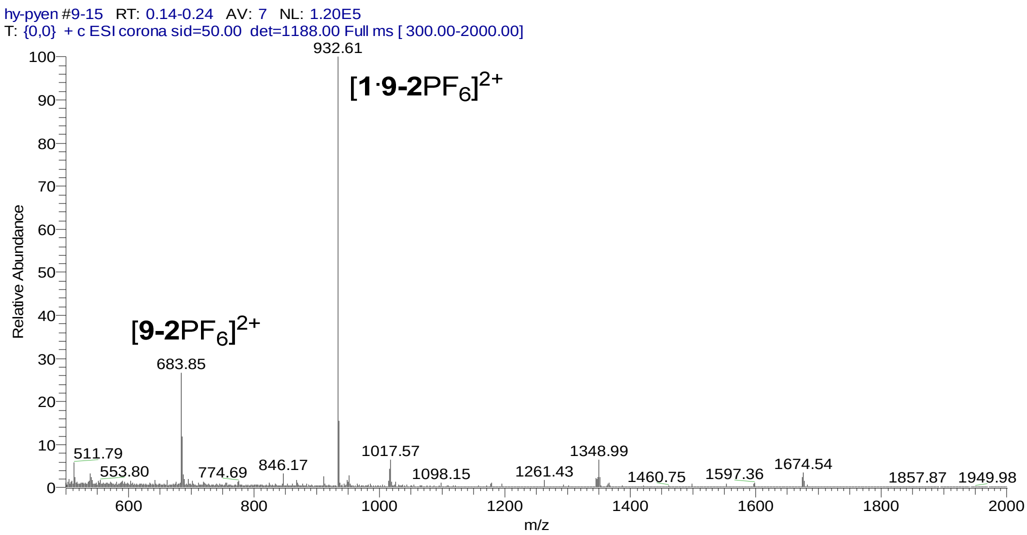

Figure S55. ESI MS of **1** and **9** in acetonitrile-chloroform (1:1, v:v).

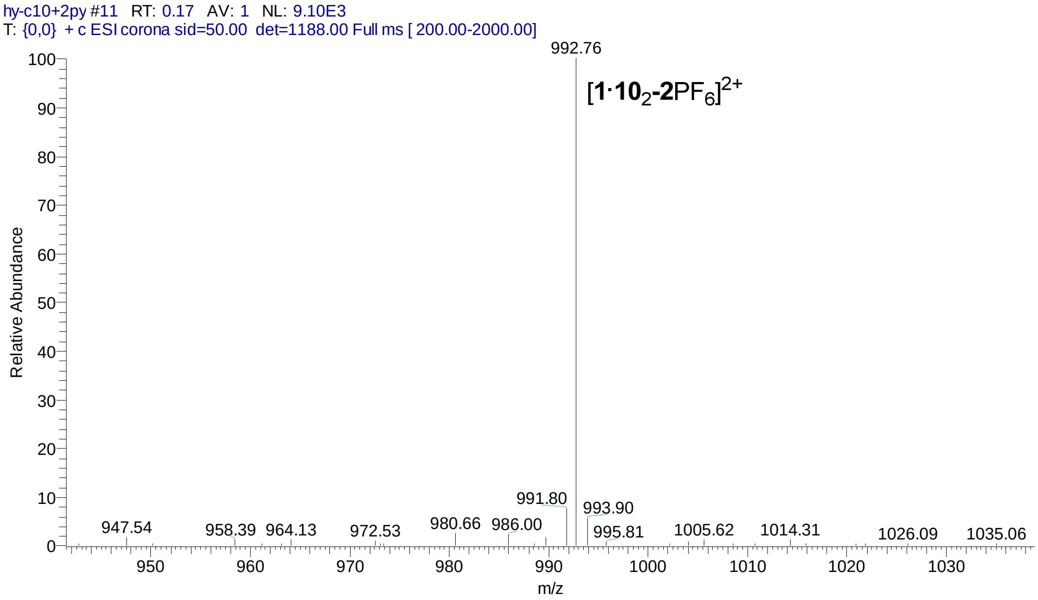

Figure S56. ESI MS of **1** and **10** in acetonitrile-chloroform (1:1, v:v).

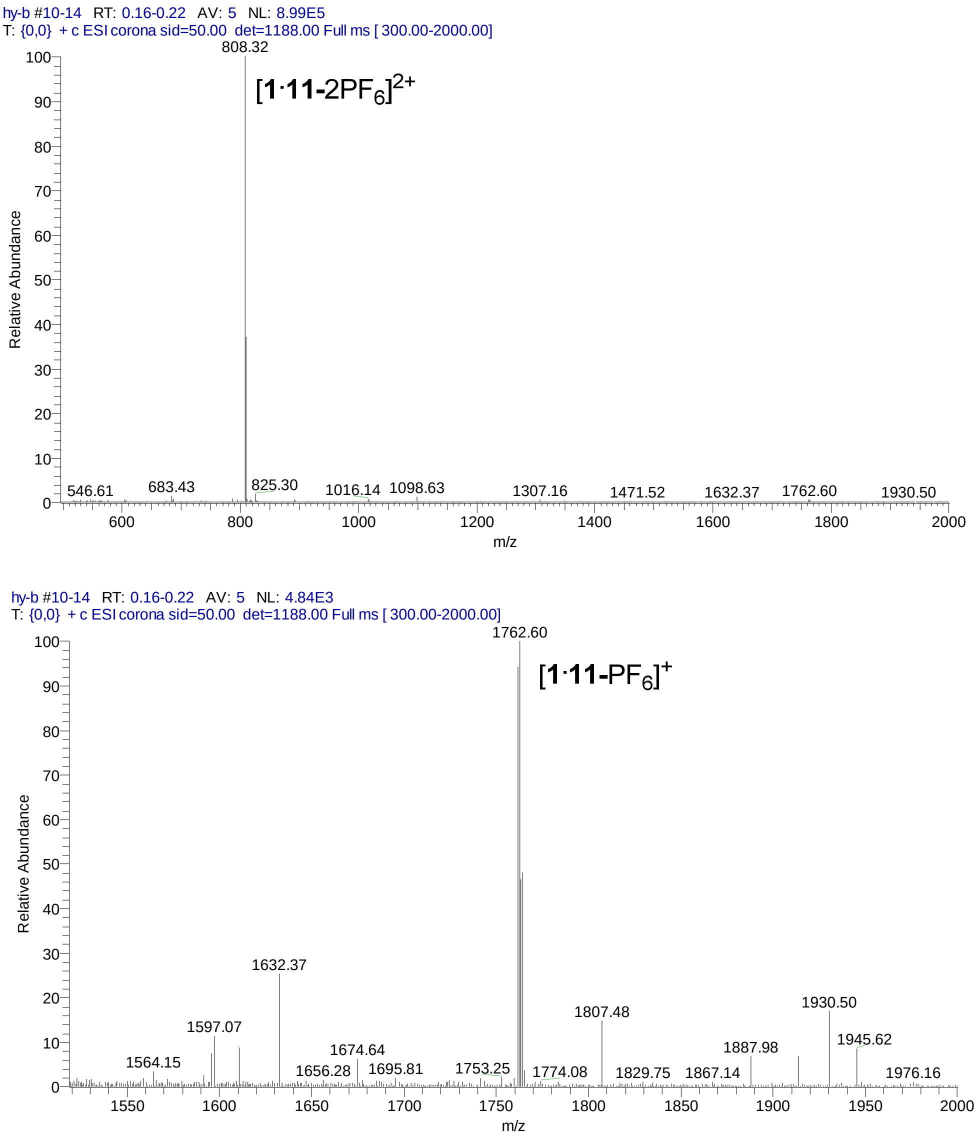

Figure S57. ESI MS of **1** and **11** in acetonitrile-chloroform (1:1, v:v).

6. Crystal structures and packing of the complexes

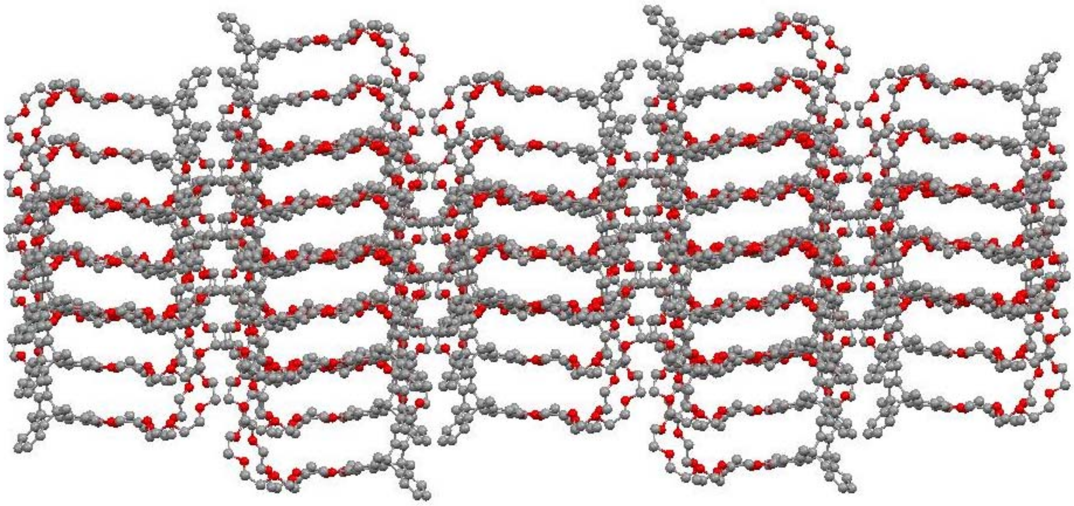

Figure S58. View of packing of host **1**. Solvent molecules and hydrogen atoms were omitted for clarity.

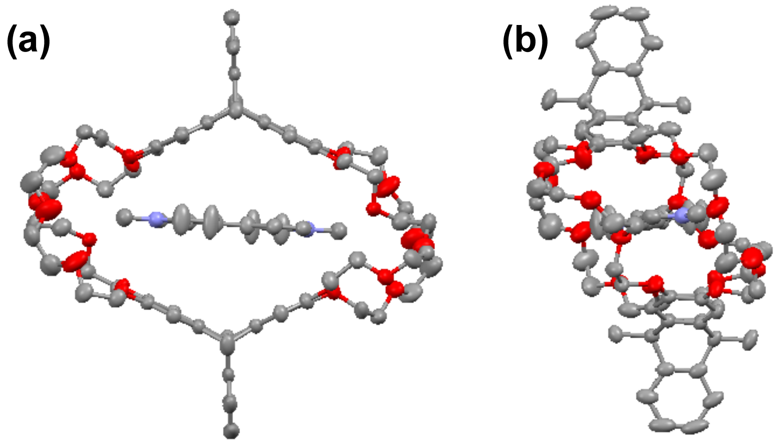

Figure S59. Side (a) and top view (b) of the crystal structure of complex **1·3**$_2$ with ellipsoid plots. PF_6^- counterions, and hydrogen atoms were omitted for clarity.

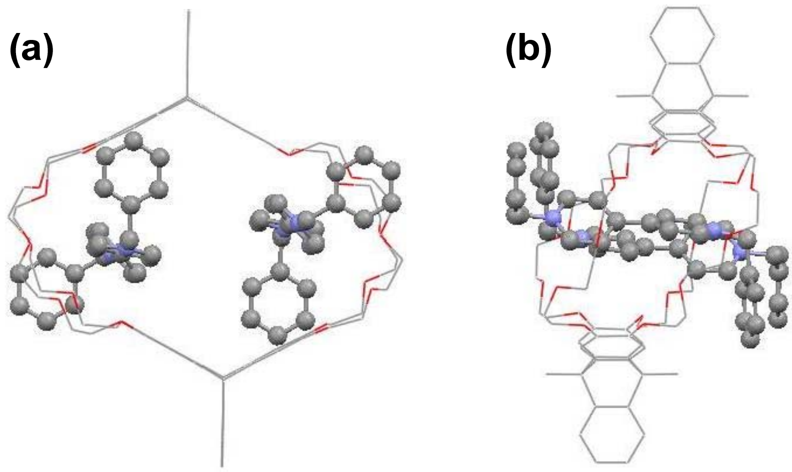

Figure S60. Side (a) and top view (b) of the crystal structure of complex **1·4**$_2$. PF_6^- counterions, and hydrogen atoms were omitted for clarity.

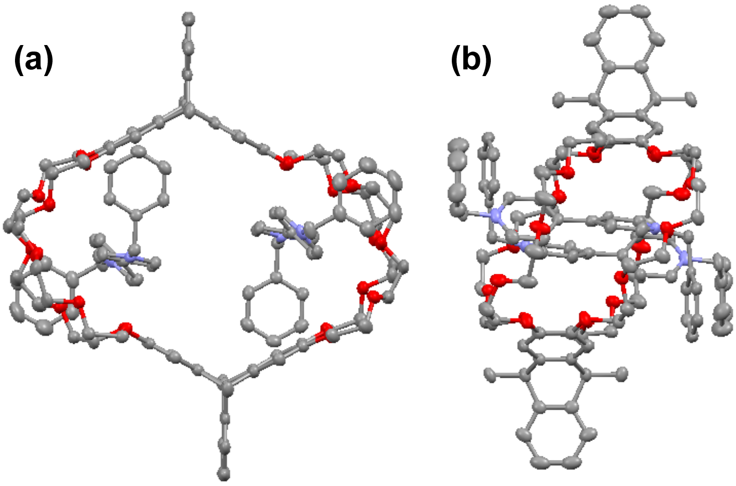

Figure S61. Side (a) and top view (b) of the crystal structure of complex **1**·**4**$_2$ with ellispoid plots. PF_6^- counterions, and hydrogen atoms were omitted for clarity.

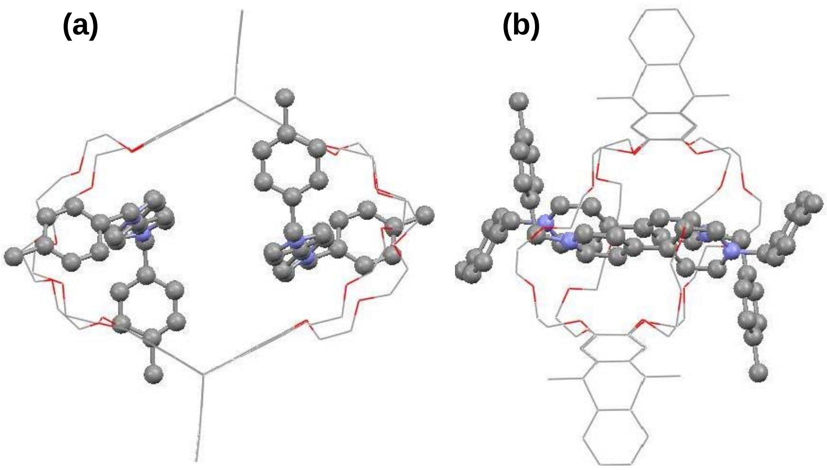

Figure S62. Side view (a) and (b) of the crystal structure of complex **1**·**5**$_2$. PF_6^- counterions, and hydrogen atoms were omitted for clarity.

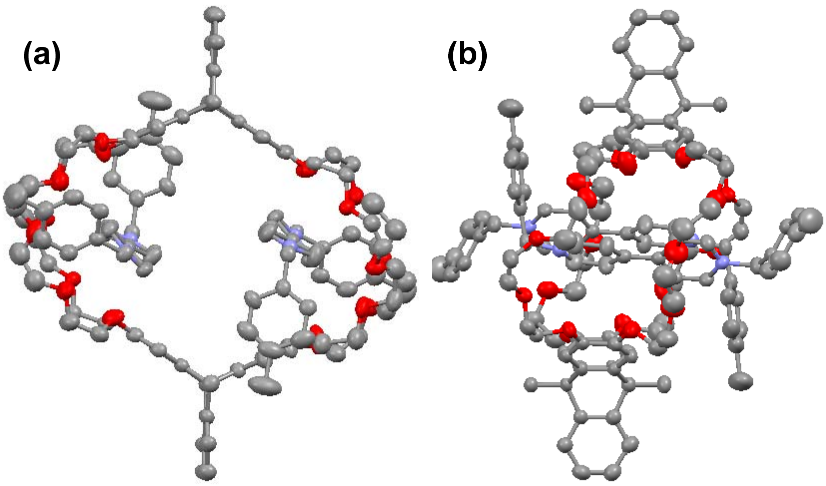

Figure S63. Side view (a) and (b) of the crystal structure of complex **1**·**5**$_2$ with ellispoid plots. PF_6^- counterions, and hydrogen atoms were omitted for clarity.

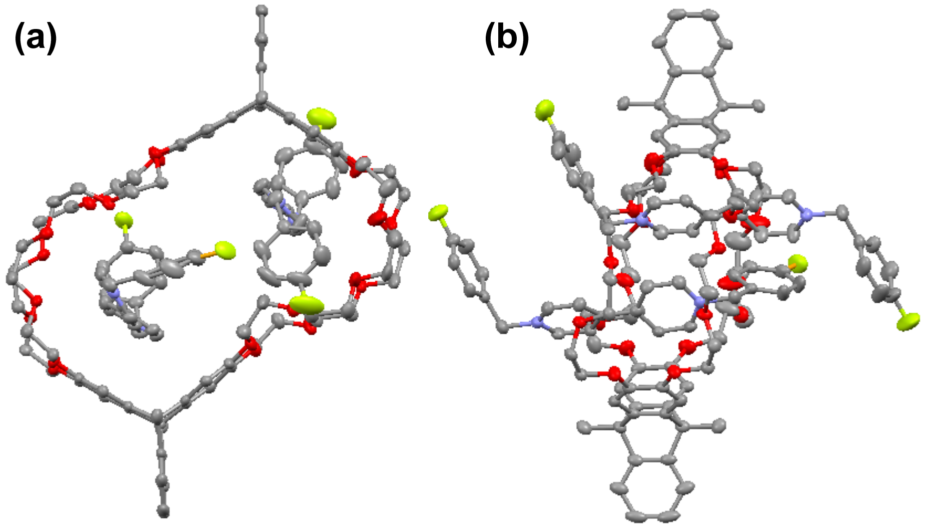

Figure S64. Side view (a) and (b) of the crystal structure of complex **1·6**$_2$ with ellipsoid plots. Solvent molecules, PF_6^- counterions, and hydrogen atoms were omitted for clarity.

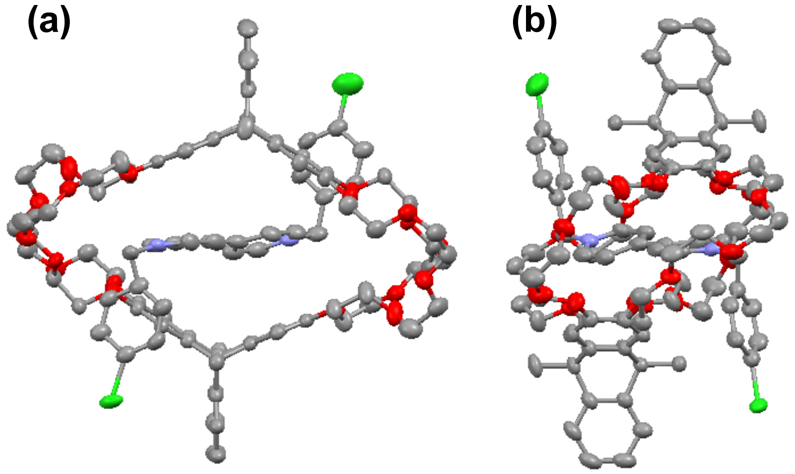

Figure S65. Side view (a) and (b) of the crystal structure of complex **1·7** with ellipsoid plots. PF_6^- counterions, and hydrogen atoms were omitted for clarity.

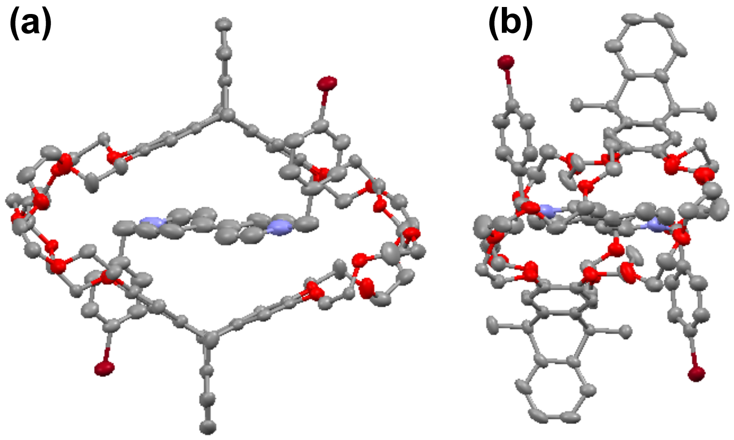

Figure S66. Side view (a) and (b) of the crystal structure of complex **1·8** with ellipsoid plots. PF_6^- counterions, and hydrogen atoms were omitted for clarity.

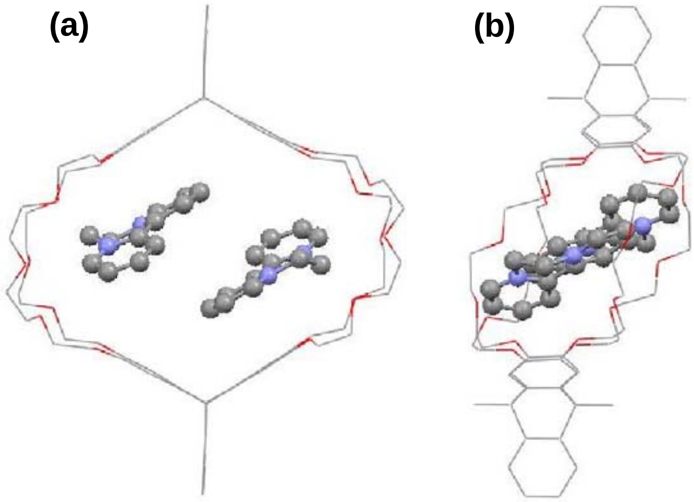

Figure S67. Side view (a) and (b) of the crystal structure of complex **1·10**$_2$. Solvent molecules, PF_6^- counterions, and hydrogen atoms were omitted for clarity.

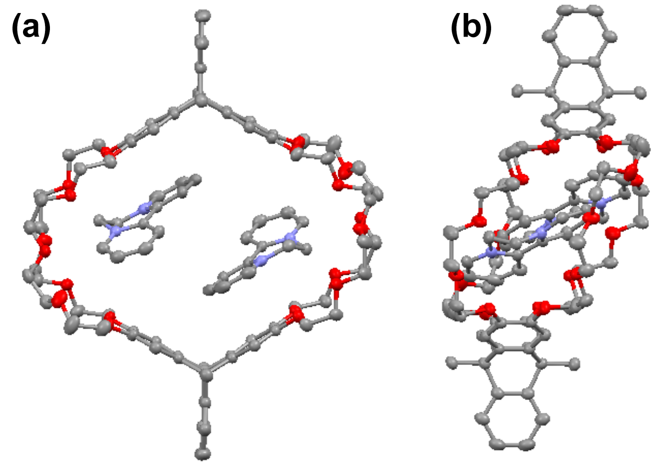

Figure S68. Side view (a) and (b) of the crystal structure of complex **1·10**$_2$ with ellipsoid plots. Solvent molecules, PF_6^- counterions, and hydrogen atoms were omitted for clarity.

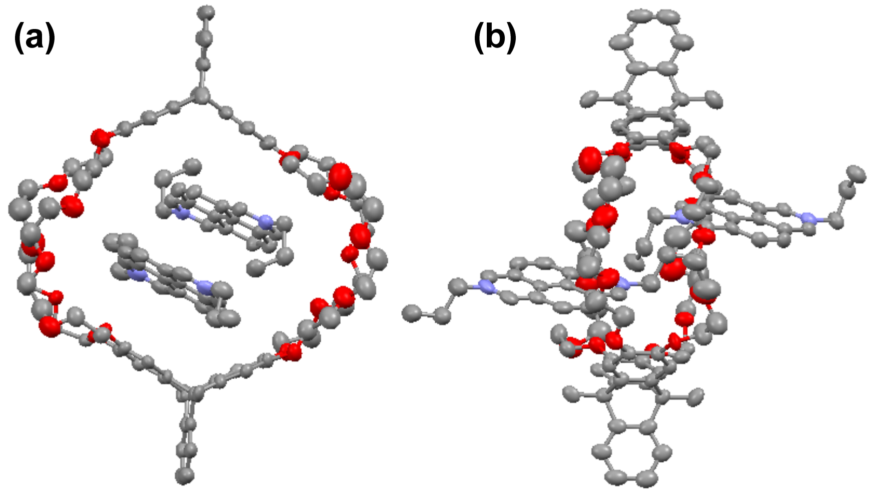

Figure S69. Side view (a) and (b) of the crystal structure of complex **1·11** with ellipsoid plots. PF_6^- counterions, and hydrogen atoms were omitted for clarity.

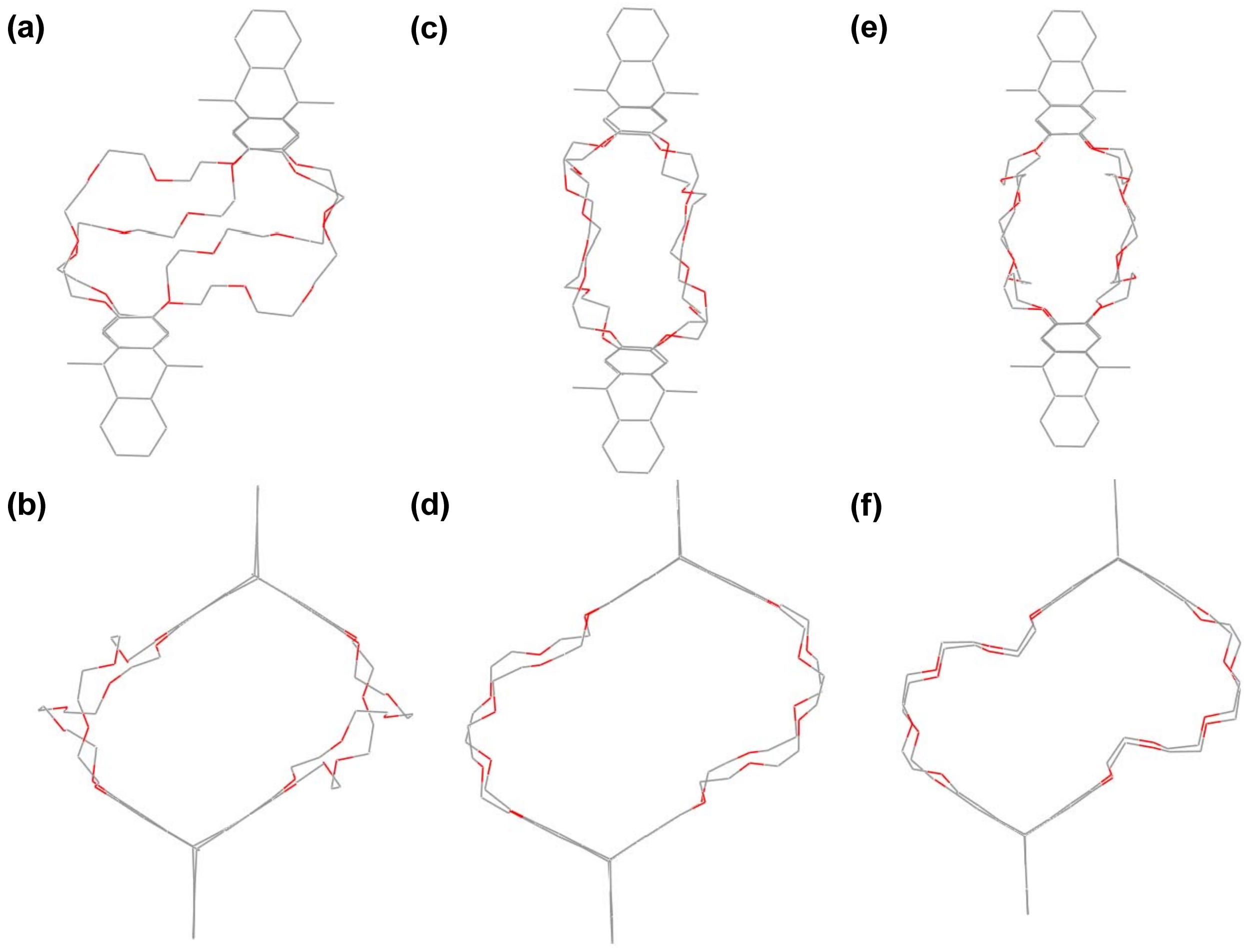

Figure S70. Crystal structures. Side view (a) and top view (b) of host **1**. Side view (c) and top view (d) of complex **1·2b**$_2$ in the absence of guests. Side view (e) and top view (f) of complex **1·2d**$_2$ in the absence of guests. Hydrogen atoms were omitted for clarity.

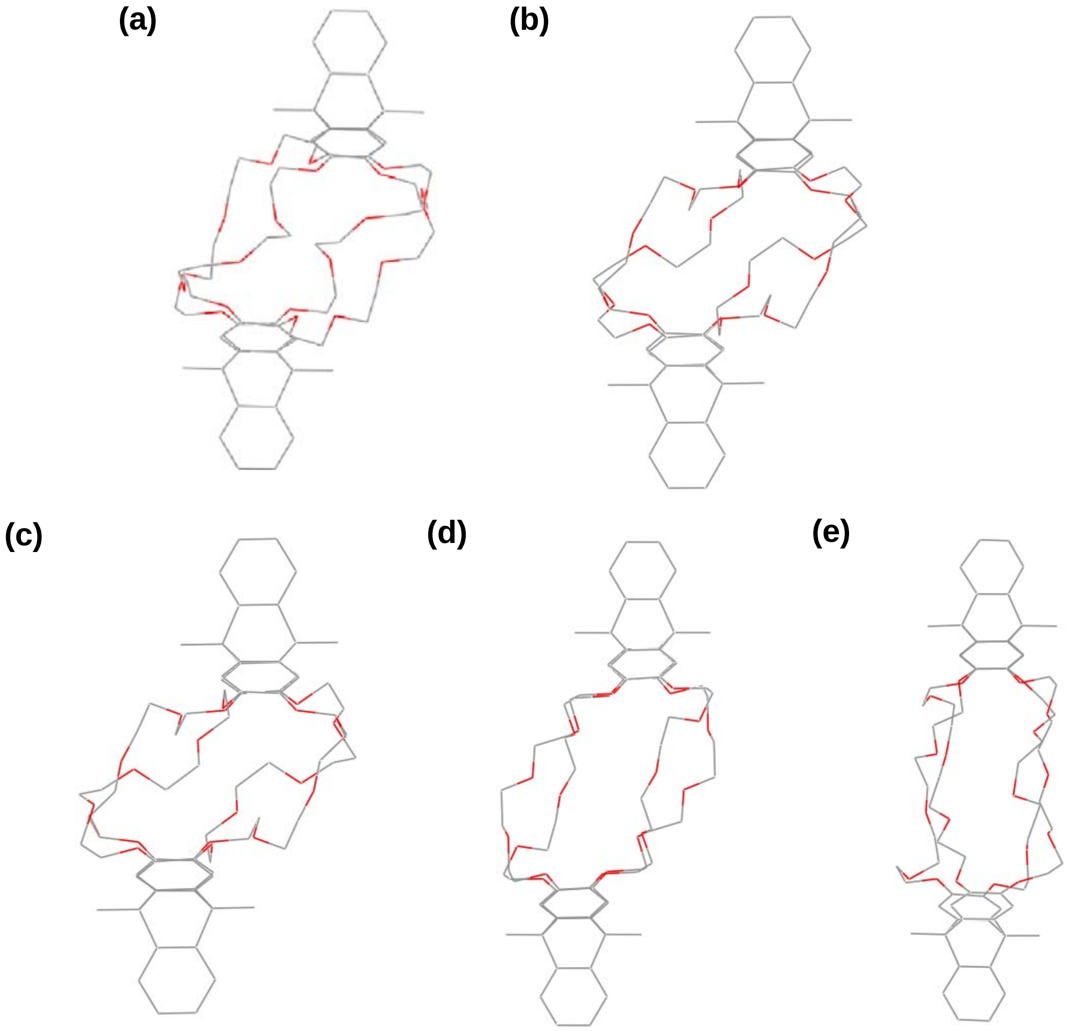

Figure **S71.** Crystal structures of the complexes in the absence of guest(s). Side views of (a) complex **1·3**, (b) complex **1·7**, (c) complex **1·8**, (d) complex **1·10**$_2$ and (e) complex **1·11**. Solvent molecules and hydrogen atoms were omitted for clarity.

7. K^+ ion-controlled binding and releasing of the guests in the complexes

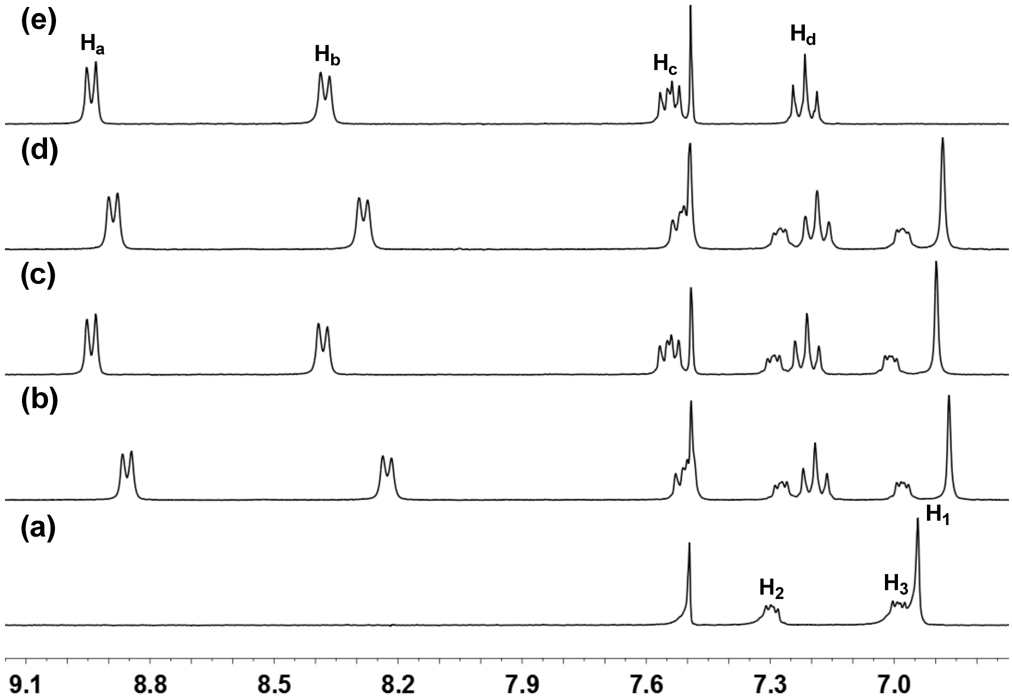

Figure S72. Partial ^1H NMR spectra (300 MHz, $CD_3CN/CDCl_3$= 1:1, v/v, 298K) of (a) free **6**, (b) **1** and 1.0 equiv. of **6**, (c) to the solution of b was added 4.0 equiv. of KPF_6, and (d) to the solution of c was added 6.0 equiv. of [18]-crown-6. $[\mathbf{1}]_0$ = 3.0 mM.

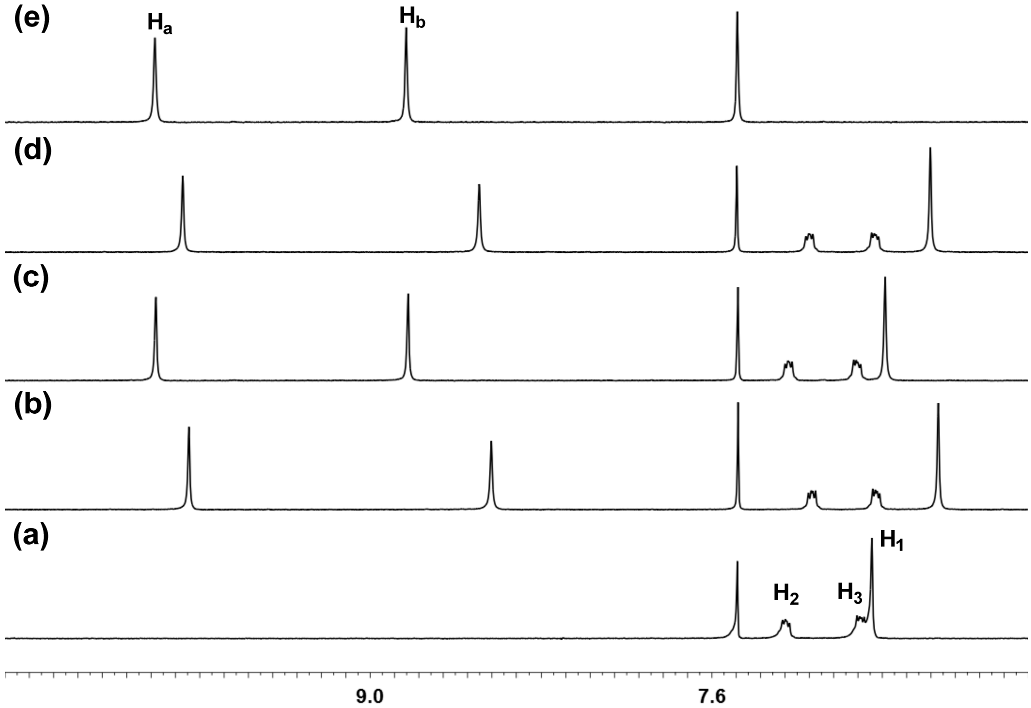

Figure S73. Partial ^1H NMR spectra (300 MHz, $CD_3CN/CDCl_3$= 1:1, v/v, 298K) of (a) free guest **11**, (b) **1** and 1.0 equiv. of **11**, (c) to the solution of b was added 4.0 equiv. of KPF_6, and (d) to the solution of c was added 6.0 equiv. of [18]-crown-6. $[\mathbf{1}]_0$ = 3.0 mM.